University of New Mexico
UNM Digital Repository

Electrical and Computer Engineering ETDs | Engineering ETDs

12-26-1963

A Study of Certain Atmospheric Effects on Radar Accuracy

Kenneth R. Swimm

Follow this and additional works at: https://digitalrepository.unm.edu/ece_etds

 Part of the Electrical and Computer Engineering Commons

Recommended Citation
Swimm, Kenneth R.. "A Study of Certain Atmospheric Effects on Radar Accuracy." (1963). https://digitalrepository.unm.edu/ece_etds/383

This Thesis is brought to you for free and open access by the Engineering ETDs at UNM Digital Repository. It has been accepted for inclusion in Electrical and Computer Engineering ETDs by an authorized administrator of UNM Digital Repository. For more information, please contact disc@unm.edu.

UNIVERSITY OF NEW MEXICO-UNIVERSITY LIBRARIES
A14429 089228

MOSPHERI
EFFECTS
ON RADAR
ACCURACY

SWIMM

378.789
Un30sw
1964
cop. 2

THE LIBRARY
UNIVERSITY OF NEW MEXICO

Call No.
378.789
Un30sw
1964
cop.2

Accession
Number
321723

IMPORTANT!

Special care should be taken to prevent loss or damage of this volume. If lost or damaged, it must be paid for at the current rate of typing.

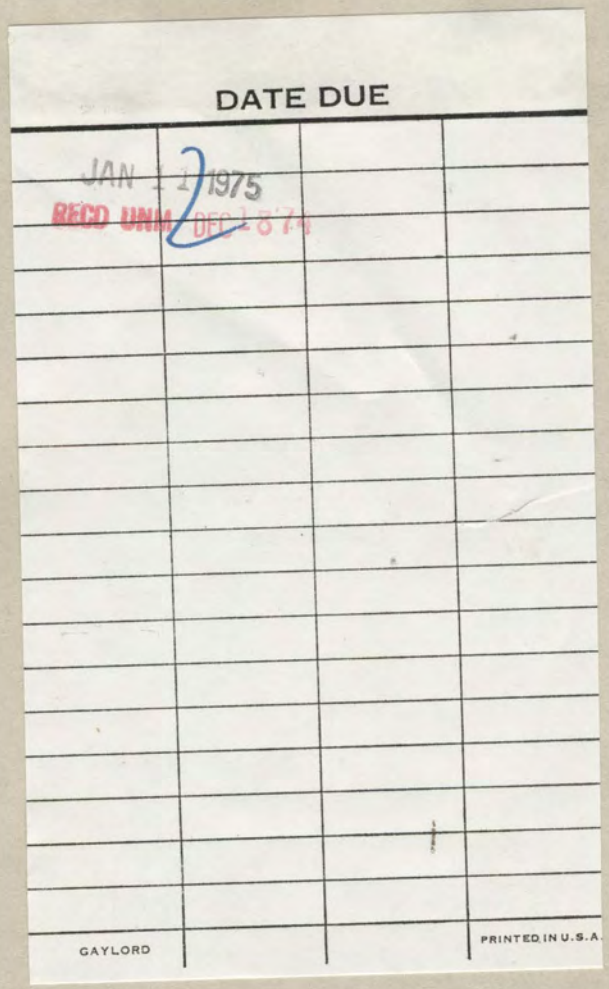

UNIVERSITY OF NEW MEXICO LIBRARY

MANUSCRIPT THESES

Unpublished theses submitted for the Master's and Doctor's degrees and deposited in the University of New Mexico Library are open for inspection, but are to be used only with due regard to the rights of the authors. Bibliographical references may be noted, but passages may be copied only with the permission of the authors, and proper credit must be given in subsequent written or published work. Extensive copying or publication of the thesis in whole or in part requires also the consent of the Dean of the Graduate School of the University of New Mexico.

This thesis by Kenneth R. Swimm
has been used by the following persons, whose signatures attest their acceptance of the above restrictions.

A Library which borrows this thesis for use by its patrons is expected to secure the signature of each user.

NAME AND ADDRESS	DATE

A STUDY OF CERTAIN ATMOSPHERIC EFFECTS ON RADAR ACCURACY

By
Kenneth R. Swimm

A Thesis
Submitted in Partial Fulfillment of the
Requirements for the Degree of
Master of Science in Electrical Engineering

The University of New Mexico
1963

This thesis, directed and approved by the candidate's committee, has been accepted by the Graduate Committee of the University of New Mexico in partial fulfillment of the requirements for the degree of

MASTER OF SCIENCE

Dean

Dec 26, 1963

Date

Thesis committee

Chairman

321723

378.789
Un 30 sw
1964
cop 2

TABLE OF CONTENTS

TABLE OF CONTENTS (Continued)

LIST OF FIGURES

LIST OF FIGURES (Continued)

CHAPTER I

INTRODUCTION

Along with other factors, accurate radar target location is dependent upon a knowledge of the electromagnetic propagation path. The propagation path is a function of the characteristics of the medium through which the signal travels. Advances in the resolution capabilities of modern electronic tracking equipment have led to requirements for more accurate prediction of atmospheric refraction characteristics. The inherent error of the equipment is, in many cases, less than the error introduced by the atmospheric refractive effects. After corrections to observed launch angle and target range have been made on the basis of atmospheric refraction information, residual errors in range and angle determination may exceed the instrumental error of the radar. The value of designing a system, perhaps at considerable expense, to provide accuracies better than the limits presently imposed by these residual errors is questionable.

While the refractive error is at present the largest limitation on accurate target location, other atmospheric effects contribute to target position error. It will be the purpose of this paper to consider the effects of atmospheric absorption and dispersion, and to determine whether they present any immediate or future problem in target location.

In Chapter II, the atmospheric effects on propagation will be broadly summarized, and refractive error correction techniques discussed.

With knowledge of the atmospheric refractive index profile, a correction to the observed target position can be made. The accuracy of the correction in angle and range is dependent upon the precision with which the appropriate index profile for the propagation path is known. Since the path index profile cannot be completely determined, there will be a residual error after the initial correction. For a target inside the atmosphere the value of the index at the target is often unknown. Outside the atmosphere the index can be assumed equal to unity, within one part in 10^6 , and the target index value is for our purposes known. This difference leads to slightly different correction schemes for targets inside and outside the atmosphere. The magnitudes of expected residual errors are considered for targets both in and out of the atmosphere. Residual errors increase as the elevation angle is decreased, the uncertainty in angular correction contributing the largest position error.

Having considered the external effects of the atmosphere, the theoretical range accuracy obtainable is analyzed. A pulsed radar makes a measurement of the time lag τ, between transmission and reception of the emitted pulse. The accuracy of this measurement is affected by the introduction of noise,

the return signal being a combination of target return and noise. In Chapter III use will be made of the probability distribution involving the transmitted and received signal to determine the theoretical limitations on accuracy.

Having received a signal which is a mixture of noise and target reflection, the problem is to operate on the returned wave shape so as to present the best obtainable value of τ, removing the ambiguity due to the inclusion of noise. For a given return signal we are interested in the probability density function of the value of time lag, τ. We define $P_y(\tau)$ as the probability of τ given y, the received signal. An ideal receiver will then present $P_y(\tau)$ to us upon receiving y at its input. Assuming Gaussian noise and high signal to noise ratios $P_y(\tau)$ is developed and the error in τ measured by the spread in $P_y(\tau)$. $P_y(\tau)$ is shown to be Gaussian as would be expected from the nature of the assumed noise, and the standard deviation is shown to be inversely proportional to the rms deviation of the energy spectrum with respect to the carrier frequency and inversely proportional to the square root of the signal to noise ratio.

In Chapter IV we will make use of our general time error expression to examine rectangular and Gaussian envelope signals with respect to their inherent rms error. These signals are analyzed to give us accuracy expressions in terms of familiar signal parameters such as bandwidth, rise time, and

pulse width.

Having developed expressions for time measurement errors in terms of these common parameters we will examine in Chapter V the effects which molecular dispersion and absorption have on these parameters, and on the wave shape itself. To do this we briefly discuss the molecular absorption and dispersion of electromagnetic waves. The only atmospheric molecules that need to be considered are water vapor and oxygen. These molecules behave as dipoles, and the reaction between the passing wave and the molecules is frequency sensitive. The introduction of a frequency sensitive velocity results in a separation of the different frequency components of the pulse as they travel along the ray path and creates a dispersion of the wave. The wave deformation caused by these dipoles is analyzed and shown to have negligible effect on the wave shape. Atmospheric attenuation is also a function of frequency and this frequency sensitive absorption alters the wave shape as the different frequency components experience different attenuations. The effect of this phenomenon is applied to a practical rectangular pulse and shown to have a negligible effect on accuracy for carrier frequencies below 30 kilomegacycles.

The most important effect of absorption on range accuracy in practical cases is shown to be the decrease in the signal to noise ratio due to the absorption of the signal rather than the deformation of the wave shape.

A comparison of the errors introduced by the atmospheric condition then indicates that the major source of error in target position is the residual angular error which is significant at extremely low angles of elevation.

CHAPTER II
GENERAL ATMOSPHERIC EFFECTS

Refraction

Refractive bending of a traveling electromagnetic wave occurs in a medium with a changing index of refraction, where

$$n = \frac{c}{v} = \left[\frac{\mu\epsilon}{\mu_0\epsilon_0}\right]^{1/2} \qquad (1)$$

n is the index of refraction

c is the speed of light

v is the phase velocity of the wave

ϵ is the permittivity of the medium

μ is the permiability of the medium

and the subscripts o refer to free space values.

The atmospheric refraction introduces a curvature in the path of an electromagnetic wave which has generally been described in terms of ray theory. The ray theory description of electromagnetic propagation can be developed from Maxwell's Equations with the assumption that the frequency is great enough to allow the neglect of certain of the terms in the formal development. The formalization of correct limitations on the use of ray theory is not available and for the purpose

of this paper the usual assumption of the applicability of ray theory to the troposhpere will be used. Experimental results indicate a general agreement with ray theory for radar frequencies, within the limitations of our present measurement capabilities. With accurate index profiles becoming more easily obtainable and actual radar measurement accuracies increasing, specification of the formal limitations on ray theory as a factor in our refraction correction schemes becomes more important.

When the index profile has been assumed to be spherically symmetrical the curvature K, of a ray path, can be determined from the scalar form of the ray equation[1].

$$K = \frac{1}{n}\left(-\frac{dn}{dR}\right) \cos i \qquad (2)$$

where n = the index of refraction

R = the radial coordinate in polar (plane) coordinates

K = the curvature of the ray at the point

i = the acute angle between the normal to R and the ray

K has been defined positive when $\frac{dn}{dR}$ is negative.

From the geometry of figure 1 where spherical symmetry has been assumed

$$K = \frac{d\Psi}{ds} = -\frac{1}{n}\frac{dn}{dR}\cos i$$

---

1. D. E. Kerr "Propagation of Short Radio Waves", Radiation Laboratory Series, McGraw Hill, Vol. 13 pages 41-46.

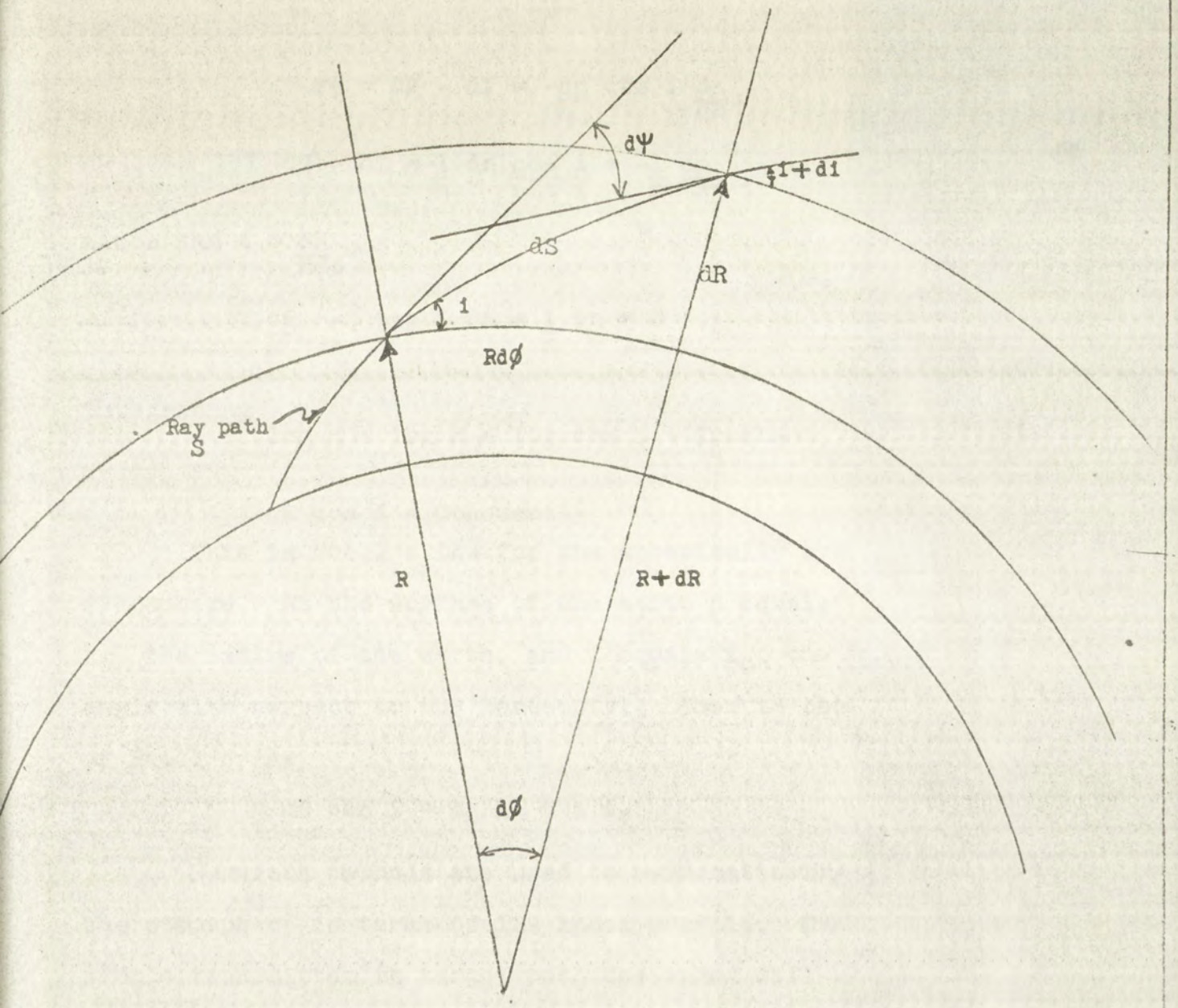

FIGURE 1

RAY TRACE GEOMETRY FOR SPHERICAL SYMMETRY

$$d\Psi = d\phi - di = \frac{-dn}{n} \cos i \frac{ds}{dR}$$

$$d\phi - di = \frac{-1}{n} dn \frac{\cos i}{\sin i} = \frac{-1}{n} \frac{dn}{\tan i}$$

since $\tan i = \frac{dR}{R d\phi}$

$$\frac{dR}{R} - \tan i \, di + \frac{1}{n} dn = 0$$

integrating

$$\log n + \log R + \log \cos i = \text{Constant}$$

or

$$nR \cos i = \text{Constant}$$

This is Snell's Law for the spherically symmetric atmosphere. At the surface of the earth n equals n_o, R equals R_o, the radius of the earth, and i equals i_o, the launch angle with respect to the horizontal. Then in the usual form of Snell's Law,

$$nR \cos i = n_o R_o \cos i_o \qquad (3)$$

Numerous methods are used to mathematically describe the atmosphere in terms of its index profile. Over any single transmitter to target path the index will vary as the result of instantaneous fluctuations which are the result of inhomogeneities in the atmosphere. Even the precise measurement of an index above the transmitter cannot predict the index profile to a long range target, particularly one at low elevation angles.

To partially correct for the refractive bending an approximate description of the atmospheric index can be used

and corrections can be applied. Any corrections made must be understood to be quite approximate. To understand the approximations made in the different types of index profiles used, we must consider the atmospheric factors which determine the variation of index. In empty space the index is unity. In the atmosphere the reaction between the atmospheric molecules and a passing electromagnetic wave changes the phase velocity of the wave. The reaction is due to the induced polarization of the gas molecules by the passing wave as well as the reorientation of molecules containing permanent dipole moments. Since the index of refraction n, is nearly unity throughout the atmosphere, it is convenient to use the factor N, defined as the refractivity.

$$N = (n-1) \times 10^6 \qquad (4)$$

The relationship between microscopic atmospheric parameters and N is given by an empirical formula. The most generally accepted values for the constants are those given by Smith and Weintraub[2], of the National Bureau of Standards.

$$N = (n-1) \times 10^6 = 77.6 \left(\frac{P}{T} + 4{,}820 \frac{e}{T^2} \right)$$

where $P = P$ = total atmospheric pressure in millibars

e = partial pressure of water vapor in millibars

T = temperature in degrees Kelvin.

---

2. E. K. Smith and S. Weintraub, "The Constants in the Equation for Atmospheric Refractive Index at Radio Frequencies", Central Radio Propagation Laboratory, National Bureau of Standards, Boulder, Colorado, Report No. 1938, September, 1952.

This expression indicates that N is not a function of frequency. This is not true as the water vapor term will vary significantly between the radio frequency and visible frequency regions. The dispersive, or frequency sensitive, effects on radar propagation will be discussed in Chapter V, and for now we will assume that the index is independent of frequency.

With this knowledge of the variation of the index with p, T, and e we can determine our index profile from some meteorological measurements. Standard weather conditions can be determined and standard profiles calculated. Generally more satisfactory data can be obtained through the use of airborne refractometers. A refractometer generally samples the atmosphere within a cavity. The resonant characteristics of the cavity depend on the index of the medium and from this information the index of refraction can be determined.

Standard Atmosphere Corrections

To determine the types of correction obtained from a standard atmosphere assumption, the following analytical expressions suggested by Campen and Cole[3] are used.

$$N_{wet} = 338 - 50.9Z + 4.39Z^2 - .245Z^3 + .0071Z^4 - .00006Z^5$$

$$N_{dry} = 262 - 25.1Z + 92Z^2 - .016Z^3 + .0001Z^4$$

Z is the height above sea level, in kilometers, with

---

3. C. F. Campen and A. E. Cole, "Tropospheric Variations of Refractive Index at Microwave Frequencies", Geophysical Directorate Air Force Surveys in Geophysics, No. 79, October, 1955.

the equations applying for Z between 0 and 10 kilometers, $N_{wet} = (N_{wet}-1)10^6$ and is representative of a saturated (100% Rel. Humidity) atmosphere at all levels. $N_{dry} = (n_d-1)10^6$ and is representative of a completely dry atmosphere (0% Rel. Humidity). Above 10 kilometers the index is assumed to decrease exponentially from the value at 10 kilometers. The validity of this assumption is somewhat questionable as complete information concerning the high altitude variation of the index is not presently available.

$$N_{wet} = N_{0wet}\, e^{-\frac{h}{25,000}}$$

$$N_{dry} = N_{0dry}\, e^{-\frac{h}{25,000}}$$

where h is measured in feet above 10 kilometers.

Once we have assumed a standard atmosphere we have to accept the inherent errors involved. The actual residual error after corrections have been made is dependent on the variation of the actual atmosphere from the assumed model. Rainey and Thorn[4] present widely used mathematical approximations and different methods of approach to the problem of correcting for refraction. An elementary correction system is indicated in Appendix A and applied to the wet and dry standard atmospheres.

---

4. R. J. Rainey and D. C. Thorn, "A Radar Refraction Correction for Symmetric and Nonsymmetric Troposphere Index Distributions", Engineering Experiment Station Technical Report No. EE 43, University of New Mexico, February, 1961.

Plots of angular errors and range errors are shown in Figures 2 and 3. The greatest errors occur for the lowest angles of propagation which in turn have the least predictable index profile over the path. From Figure 2, the difference between range corrections for the wet and dry atmosphere is less than 10 feet. It must be emphasized that this figure is based on our assumption of a theoretical set of index profiles and cannot be taken too seriously. It does give us a feeling for the small magnitude of the range error when compared to the error introduced by the angular deviation. Our angular errors for low elevation angles are in the order of several milliradians. The position error in feet due to a bending of 2.3 milliradians in a wet atmosphere at an angle of 5 degrees and an altitude of 100,000 feet is

$$\Delta R_{\alpha} = R\Delta i$$

Assuming an average correction is made between the wet and dry limits, the possible error is still ± .3 milliradians and an indeterminacy of

$$.3 \times 10^{-3} \times 1{,}150{,}000 = \pm 345 \text{ ft.}$$

This will increase appreciably as the elevation angle is decreased.

The conclusions to be drawn are that in order to come close to an accurate radar's capability, the corrections must be made, and even then, an average correction based on a

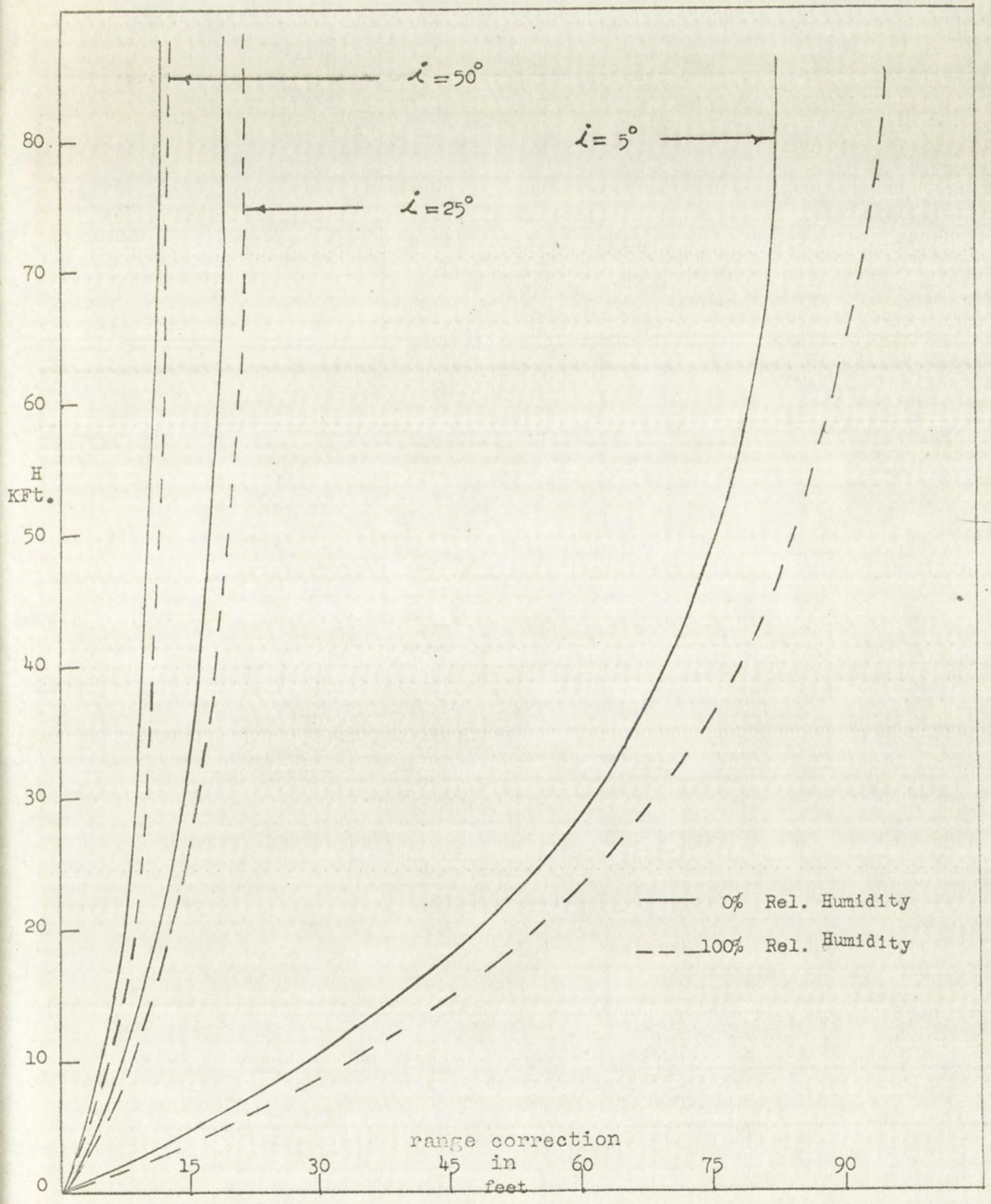

FIGURE 2
RANGE CORRECTIONS FOR TARGET HEIGHT IN 0% AND 100%
RELATIVE HUMIDITY STANDARD ATMOSPHERES

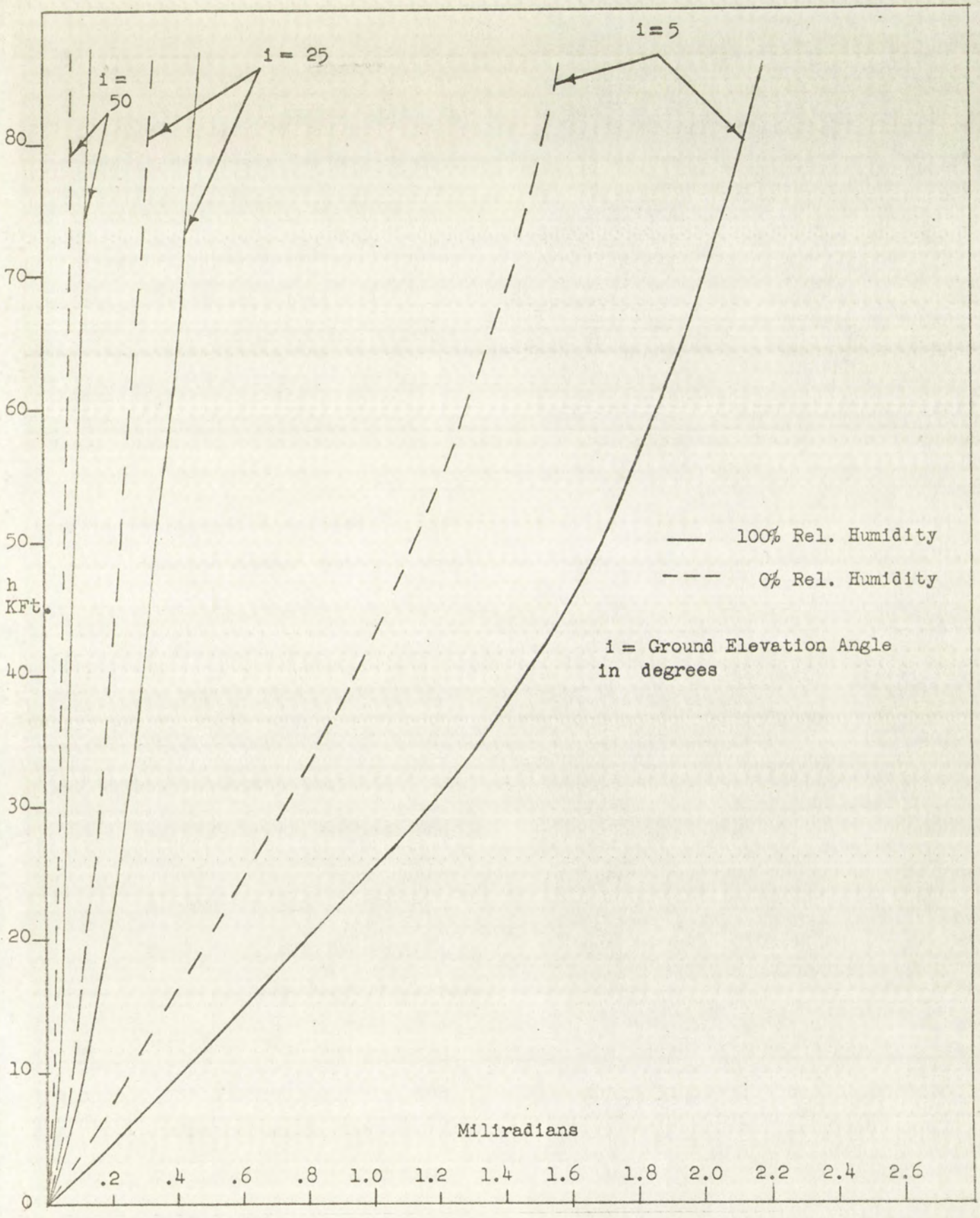

FIGURE 3

ANGULAR CORRECTIONS FOR 0% AND 100% RELATIVE HUMIDITY STANDARD ATMOSPHERES

standard atmosphere does not reduce the errors in angle resolution to the point where we can fully utilize the radar's inherent accuracy for low angles of elevation. Therefore, more accurate index profile information must be made available for reliable tracking. The error in position of the target introduced by angular change is much more influential than that in range due to the variation in speed of the signal along the path. This has been confirmed by previous investigations of The University of New Mexico.[5,6,7]

Tracking of Targets Outside the Atmosphere

Recent radar systems have been developed for satellite and high altitude missile tracking where the targets are outside the atmosphere. The situation here is slightly different for while the profile along the path is generally unknown, both end points of the index profile are available The index at the transmitter is easily available and above 200K ft., the index approaches unity to within one part in 10^{-6}.

---

5. R. Rainey and D. Thorn, "A Radar Refraction Correction for Symmetric and Nonsymmetric Troposphere Index Distributions," Engineering Exp. Sta. Tech. Report EE 43, University of New Mexico.

6. W.L. Anderson, N.J. Beyers and B.M. Fannin, "Comparison of Computed with Observed Atmospheric Refraction", IRE Transactions on Antennas and Propagation, Vol AP-7, No.3 July, 1959.

The method to be examined here follows P.F. von Handel and F. Hoehndorf.[8] Exponential variations in index are assumed and Figure 4 indicates two different paths followed by rays which encounter different index profiles.

While the diagram is exaggerated, it shows the decrease in the residual angular error ($\Delta\alpha_1 - \Delta\alpha_2$) as the distance to the target is increased past 200K ft. One immediate question is the justification of the exponential index. We will discuss the limitations involved in choosing a model for the index after outlining the mathematics used to determine the theoretical error due to refraction. Figures 5 and 6 describe the geometrical picture of the path with h_o the height above sea level of the transmitter, s the actual path, and d the straight line distance, the remainder of the parameters being self explanatory. From Figure 5

$$ds = dh/\cos \qquad (6)$$

and substituting from (3) which is still applicable after a slight modification

---

7. W.L. Anderson, N.J. Beyers, and R.J. Rainey, "Comparison of Experimental with Computed Trophospheric Refraction", IRE Transaction on Antennas and Propagation, Vol. AP-8 No. 5, September 1960

8. P.F. von Handel and F. Hoehndorf, "High Accuracy Electronic Tracking of Space Vehicles, "IRE Transaction on Military Electronics, MIL. 3, No. 4, October, 1959.

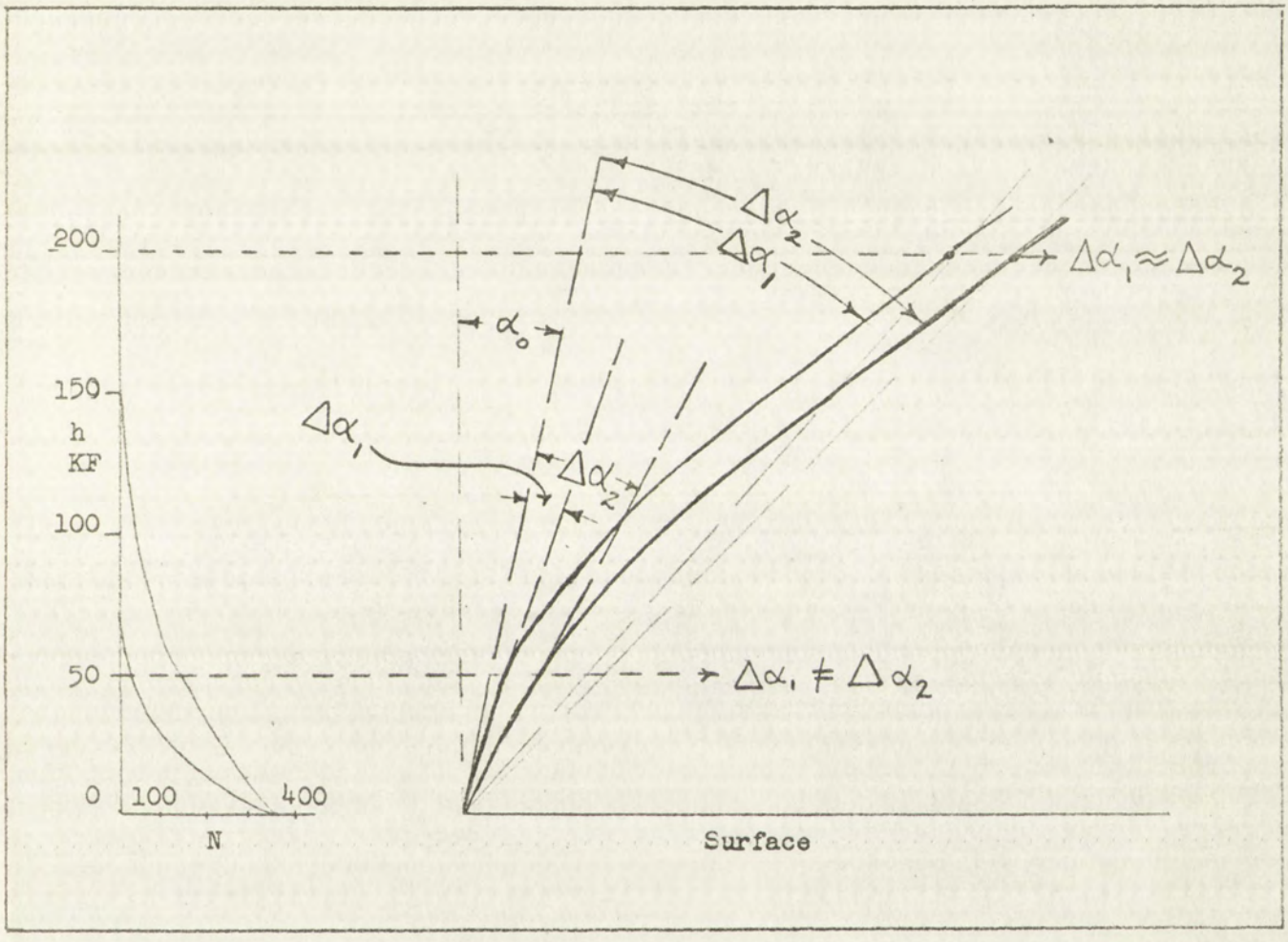

FIGURE 4

ILLUSTRATION OF RAY PATHS EXPERIENCING
DIFFERENT INDEX PROFILES

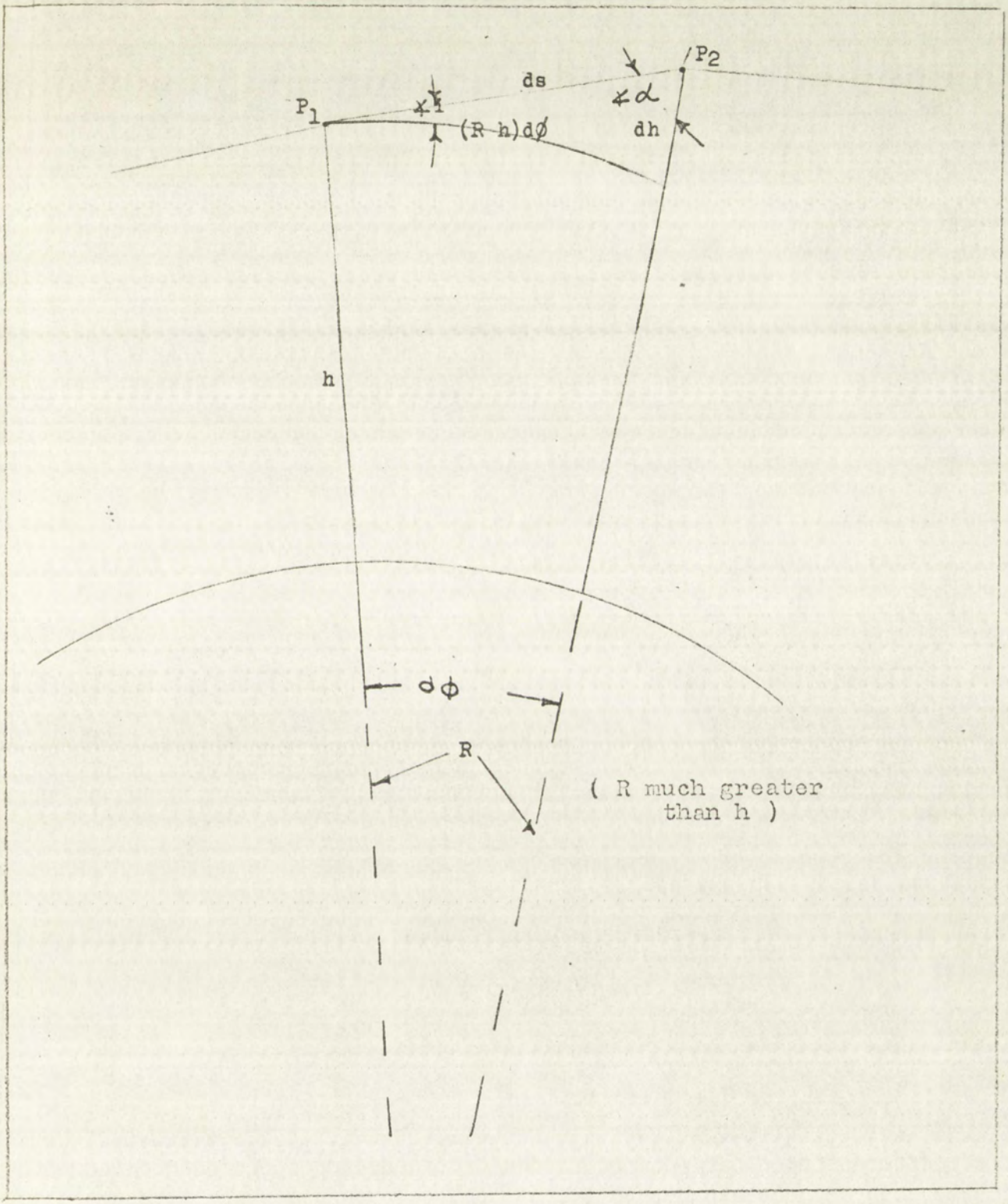

FIGURE 5

ILLUSTRATION OF RAY PATH BENDING

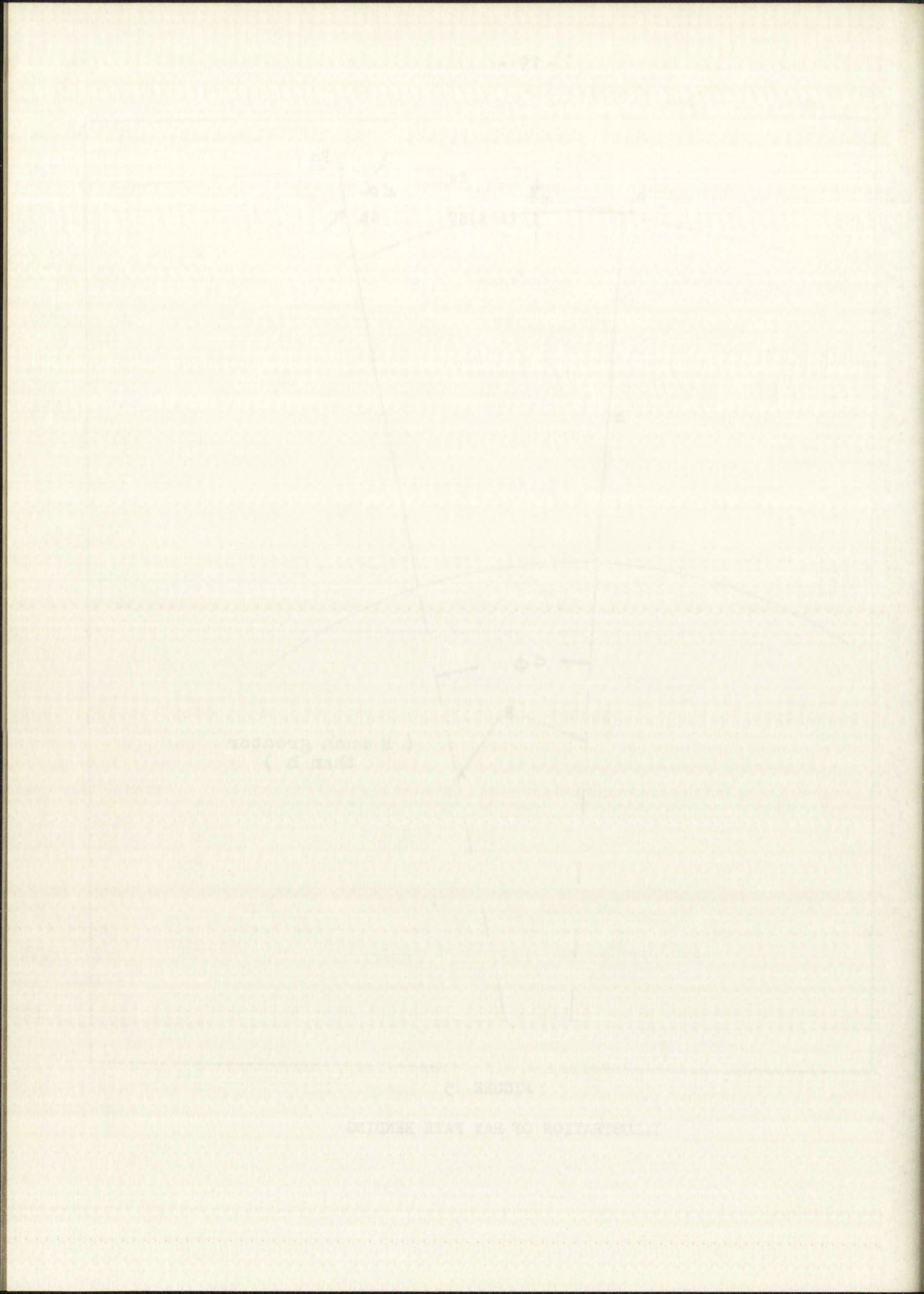

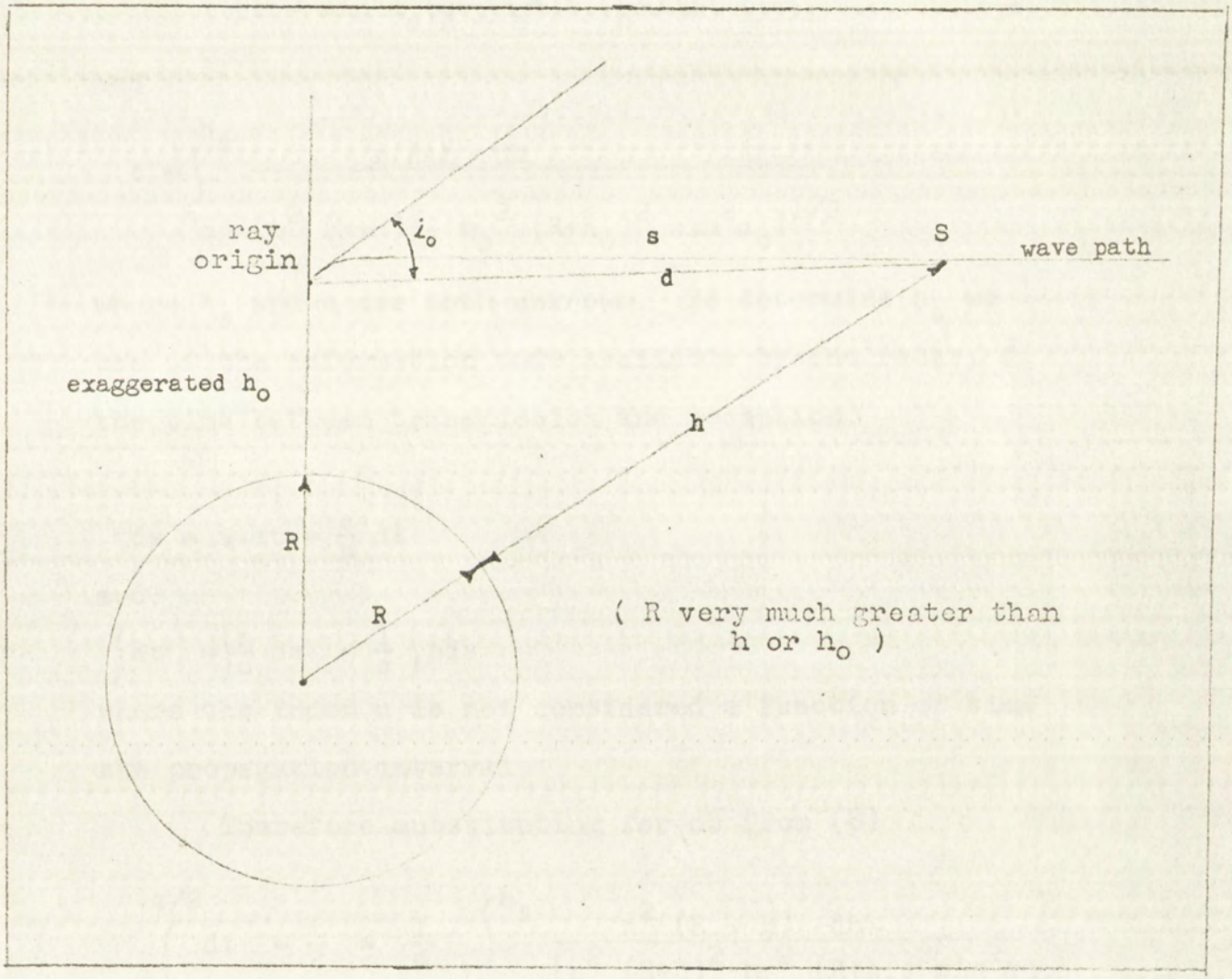

FIGURE 6

ILLUSTRATION OF RAY PATH BENDING FROM PATH
ORIGIN ABOVE SEA LEVEL

$$\cos\alpha = [1-\sin^2\alpha]^{1/2} = [1-\sin^2\alpha_o(\frac{R+h_o}{R+h})^2(\frac{n_o}{n})^2]^{1/2} \quad (7)$$

Substituting in (6) for cos

$$ds = \frac{dh}{[1-\sin^2\alpha_o(\frac{R+h_o}{R+h})^2(\frac{n_o}{n})^2]^{1/2}}$$

and

$$s = \int_{h_o}^{h_s} \frac{n(R+h)\,dh}{[n^2(R+h)^2 - n_o^2(R+h_o)^2\sin^2\alpha_o]^{1/2}} \quad (8)$$

where h_s and s are both unknown. To determine h_s we make use of the information made available by the radar, i.e., the time between transmission and reception.

$$ds = v\,dt = \frac{c}{n}\,dt$$

and

$$\int dt = \int \frac{n}{c}\,ds = \frac{1}{c}\int nds$$

where the index n is not considered a function of time over the propagation interval.

Therefore substituting for ds from (8)

$$\int_o^{\tau/2} dt = \frac{\tau}{2} = \frac{1}{c}\int_{h_o}^{h_s} \frac{n^2(R+h)\,dh}{[n^2(R+h)^2 - n_o^2(R+h_o)^2\sin^2\alpha_o]^{1/2}}$$

Only h_s is unknown in this equation and can be solved for by numerical integration if a suitable expression for n is available. We in turn can then determine s from (8). Having determined h_s, and s, then d from Figure 6 is obtained by application of the law of sines or cosines.

$$d = [(R+h_o)^2 + (R+h_s)^2 - 2(R+h_o)\,(R+h_s)\cos\phi_s]^{1/2} \qquad (11)$$

ϕ_s is still unknown, but from Figure 5

$$\tan\alpha = \frac{(R+h)}{dh}\,d\phi$$

$$\phi = \int_{h_o}^{h_s} \frac{\tan\alpha}{R+h}\,dh \qquad (12)$$

$$|\phi_s| = \int_{h_o}^{h_s} \frac{n_o\,(R+h_o)\sin\alpha_o \quad dh}{[(R+h)\,n^2\,(R+h)^2 - n_o^2\,(R+h_o)^2\sin^2\alpha_o]^{1/2}}$$

d is now calculated from (11) and the R between computed and observed range computed

$$\Delta R = d - s_a$$

where s_a is the range reading given by the radar.

$\Delta\alpha$ from Figure 6 is

$$\Delta\alpha = \sin^{-1}\left[\frac{(R+h_s)\sin\phi_s}{d}\right] - \alpha_o$$

Different index profiles of the type shown in Figure 7 were then placed into integral expressions and the differences in correction for range and angle considered.

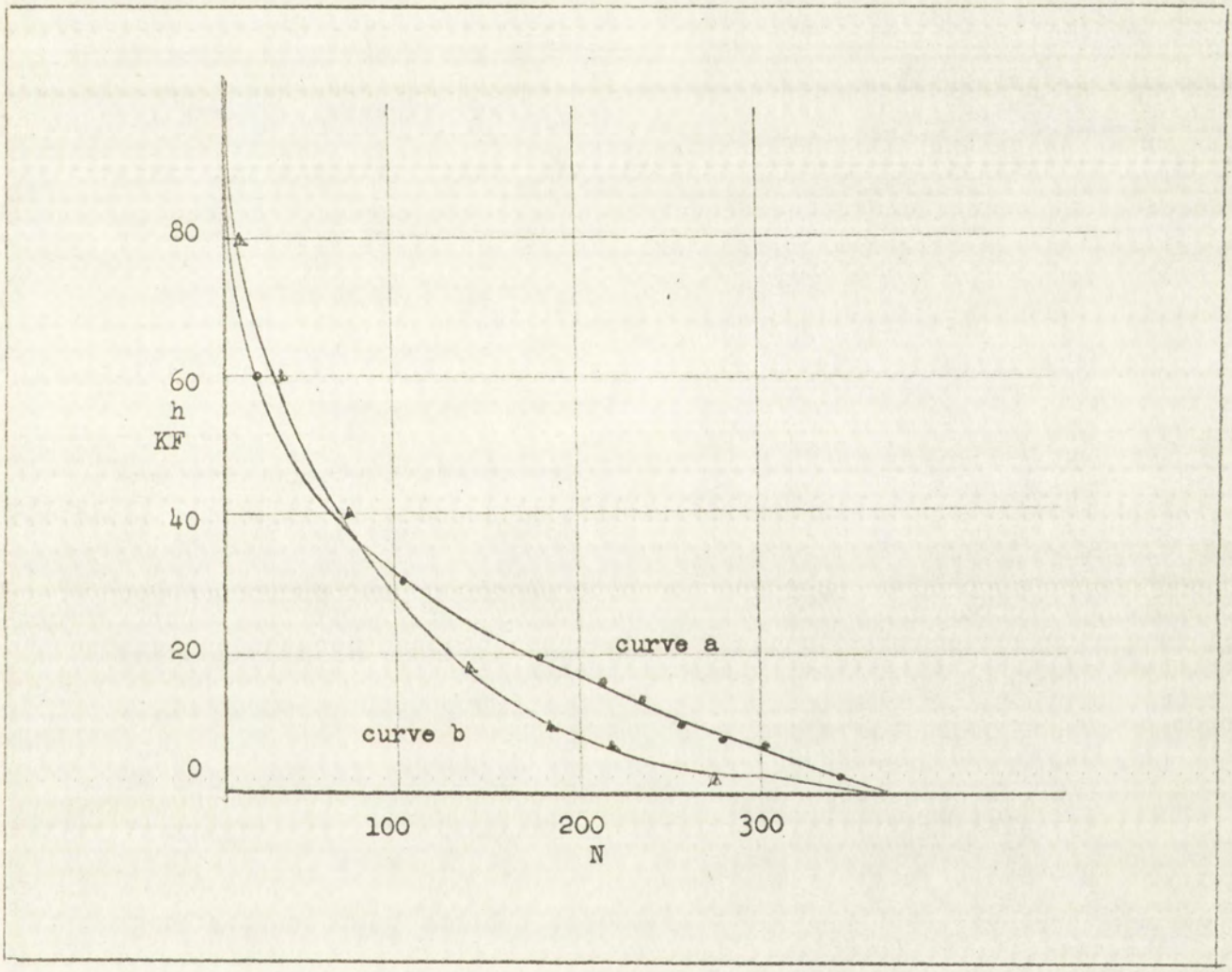

FIGURE 7

INDEX PROFILES FOR VARYING WEATHER CONDITIONS
HAVING THE SAME N_o

Figure 8, Curve b is the result of assuming extremely dry air down to 1,000 feet and then an extremely rapid humidity increase from there down to sea level. This curve could also represent a temperature inversion up to 1,000 feet in altitude. Cases representing maximum, minimum and average N_o conditions were evaluated in the integrals. The difference between the target location using the maximum and then the minimum index description was in the vicinity of 10 feet and 9 seconds of arc (0.5 milliradians) where the assumed straight line range chosen was 4,864 K ft. and the elevation angle almost 8°.

With spherical symmetry assumed the actual value of the average correction depends almost entirely on the angle of launch and the value of N_o at the transmitter, not the way in which the intermediate levels are stratified. This information is used to justify the adoption of a "standard" profile which would be simple to manipulate mathematically. An exponential decrease in N was developed of the form

$$N = N_o^{-h/H_s} \tag{15}$$

from a good many actual soundings, with an admitted deviation in the value of H around the standard value. Corrections were then determined, and the residual error due to the difference between using the standard H_s and H_s plus the maximum deviation were computed.

Figure 8 shows a graph of the residual angular errors

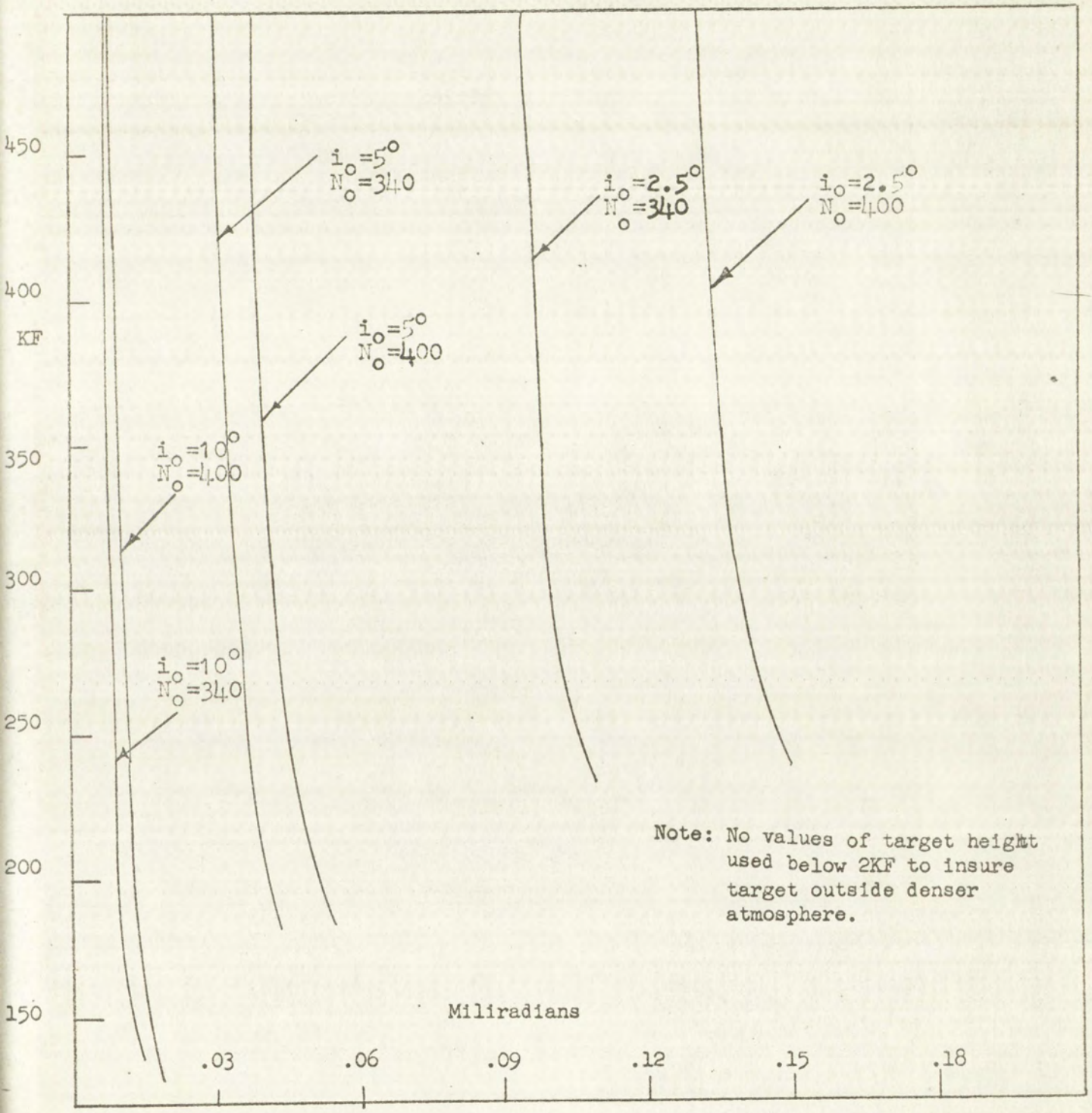

FIGURE 8

RESIDUAL ANGULAR ERROR

with range. The residual range errors are all less than 10 feet and comparatively negligible.

The results of this analysis indicate that targets outside the atmosphere can be tracked within the limits of our present equipment for elevation angles greater than 2.5°. This analysis is based on the assumption of a spherically symmetric index profile. The atmospheric index profile is not spherically symmetric, but corrections made using the symmetrical model are often satisfactory[9]. Unfortunately local weather conditions can seriously disrupt the approximately symmetrical nature of the index distribution contributing a more severe error in target position. In general the difficulties involved in obtaining complete index information necessitate the use of the spherical symmetry assumption. Once this assumption is made it is emphasized that the use of non-standard profiles in the equations had the same effect on the spread of the angular corrections for these targets as did the use of extreme exponential index profiles. The extreme exponential profiles were chosen so as to form outer boundaries for the index variations that might be expected to occur. This in turn gave us the maximum variation in target location error

At elevation angles in the vicinity of 2°, a ray will

9. R. Rainey and D. Thorn, Op Cit., pp 34-35.

traverse several hundred miles in the active trophosphere. Complete weather data for index profiles over this range would be extremely difficult to obtain, especially if the entire 360° in azimuth had to be considered.

In view of this, the assumption of an exponential index for tracking targets outside the trophosphere is probably the best we can do and as demonstrated above is quite satisfactory for targets at elevation angles greater than 2.5°.

The University of New Mexico findings for targets within the troposphere showed conclusively a direct correlation between improved weather data and improved corrections. The rms error for the combined data was .28 milliradians where the true elevation angle was 17.996 milliradians and the slant range to the target was 237.18 K ft. At these low angles, the weather information becomes even more important. Even with fairly extensive weather data available, the meteorological uncertainties led to errors greater than the inherent accuracy of the AN/FPS-16 radar (C band) used.

In this experiment, for the low angle involved, the use of a surface refractive index and an exponential profile showed a generally insignificant improvement over the use of a standard atmosphere.

We find then for radar tracking, that our main concern is with extremely small elevation angles where the noncorr-

ectable angle errors will be of the order of tenths of a milliradian and the noncorrectable range errors less than 50 feet, assuming we use adequate index information.

The methods of Fannin-Jehn, and Rainey-Thorn provide as much accuracy as necessary on the basis of presently available index information. The Rainey-Thron method has the advantage of not having to assume a spherically symmetric profile. Since both methods are based on ray theory, they may not accurately describe the refractive effect when ray theory breaks down. Ray theory approximates electromagnetic propagation at high frequencies but the limits of the approximation have not presently been specified.

Ionospheric Effects on Propagation

Since this paper is concerned mainly with trophospheric propagation, we will only briefly outline the effects of the ionosphere on propagation. The ionosphere has an advantageous effect on ground to ground communications, in that propagation beyond line of sight becomes possible due to signal reflection. In tracking any target in or outside the ionosphere, the transmitted signals are reflected or bent depending on their frequency characteristics. Frequencies below the so called critical frequency are, for the most part, reflected by the ionospheric layers. Various observations of the seasonal, diurnal and sporadic variations of this critical frequency have been made with the upper limit plac-

ed in the vicinity of 80 Mc. One of the assumptions of the previous method for tracking a target outside the atmosphere was the use of frequencies in the KMC range in order to avoid ionospheric effects. Ray bending by the ionosphere is frequency sensitive and has a maximum on the order of several milliradians depending on the ionospheric conditions, and the angle of incidence. The angular deviation falls off as $\frac{1}{f^2}$ and therefore decreases rapidly with frequency. The presence of the earth's magnetic field sometimes causes a double refraction of the incident wave. The phase relationship between the two components of the wave is constantly changing. Upon leaving the ionosphere, the waves combine, the polarization of the emerging wave being different from that of the original. This decouples the receiving and transmitting antenna unless special techniques are used, and manifests itself in an effective power loss (Faraday Loss).

Noise Considerations

As we will show in Chapter IV, the accuracy or sensitivity of a radar system is limited by its overall noise content. Noise will be generated both within the set and externally by the natural sources, such as the sun. Figure 9 is taken from Pratt[10], and indicates the distribution of

10. H.J. Pratt, "Progation, Noise, and General Systems Considerations in Earth-Space Communications", IRE Transactions on Communications Systems. Vol CS-8, No.4 December, 1960.

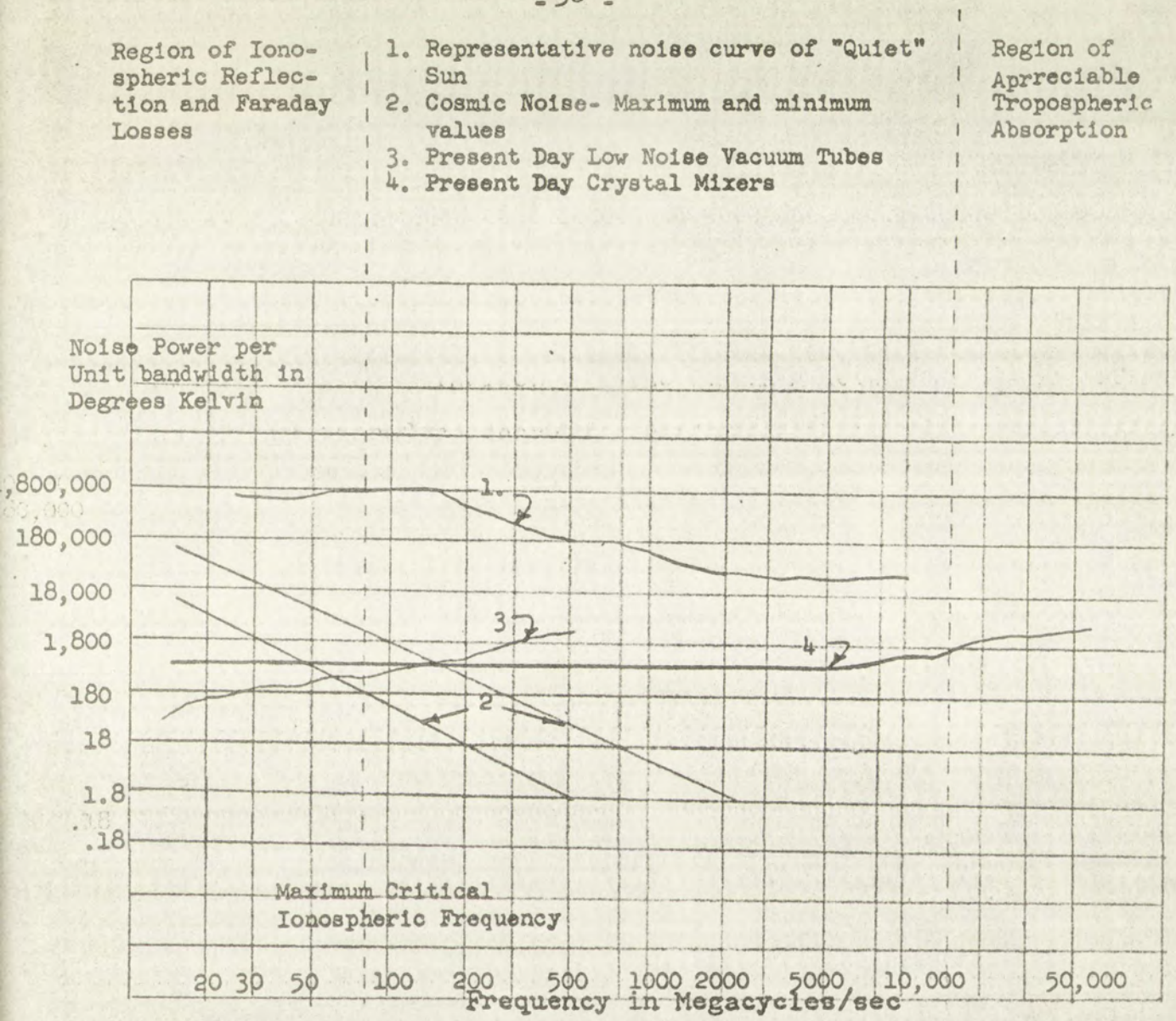

FIGURE 9

INTERNAL AND EXTERNAL SYSTEM NOISE FIGURES

both internal and external noise sources. The ordinate is the equivalent noise temperature, or noise power per unit bandwidth, and the abcissa is frequency in megacycles. Over any reasonable frequency interval, it can be seen that approximately, the noise power is equally distributed over the involved frequencies.

Trophospheric Absorption

Losses in excess of the normal attenuation with range occur in the high KMC frequency range due to molecular absorption by oxygen, uncondensed watervapor and scattering from precipitation particles. The total absorption will depend on the path length in the absorptive medium, and therefore the angle of elevation. Figure 10 shows the characteristics of tropospheric absorption with frequency. One of the purposes of this paper is to determine whether the effects of molecular dispersion and absorption at high frequencies present any immediate or future limitations for accurate radar tracking. The characteristics of scattering by fog, rain, etc., are normally insignificant below 8 KMC and can always be neglected below 1 KMC[11].

Conclusions

The rather general analysis indicates that the atmosphere is very nearly transparent between 80 Mc and 15 KMC.

---

11. Kerr, Op Cit., pp 684-688.

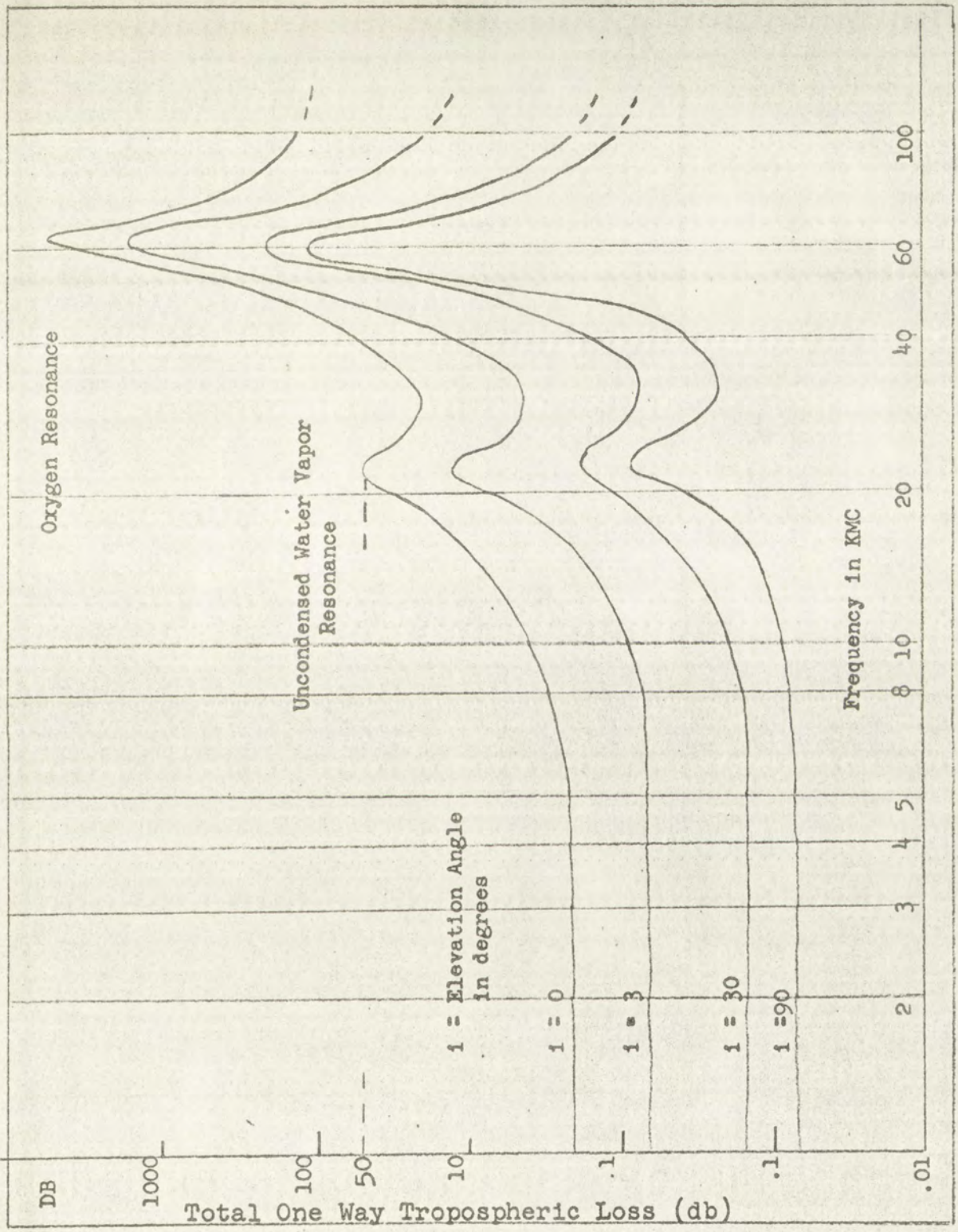

FIGURE 10

TOTAL ONE-WAY TROPOSPHERIC ABSORPTION LOSS

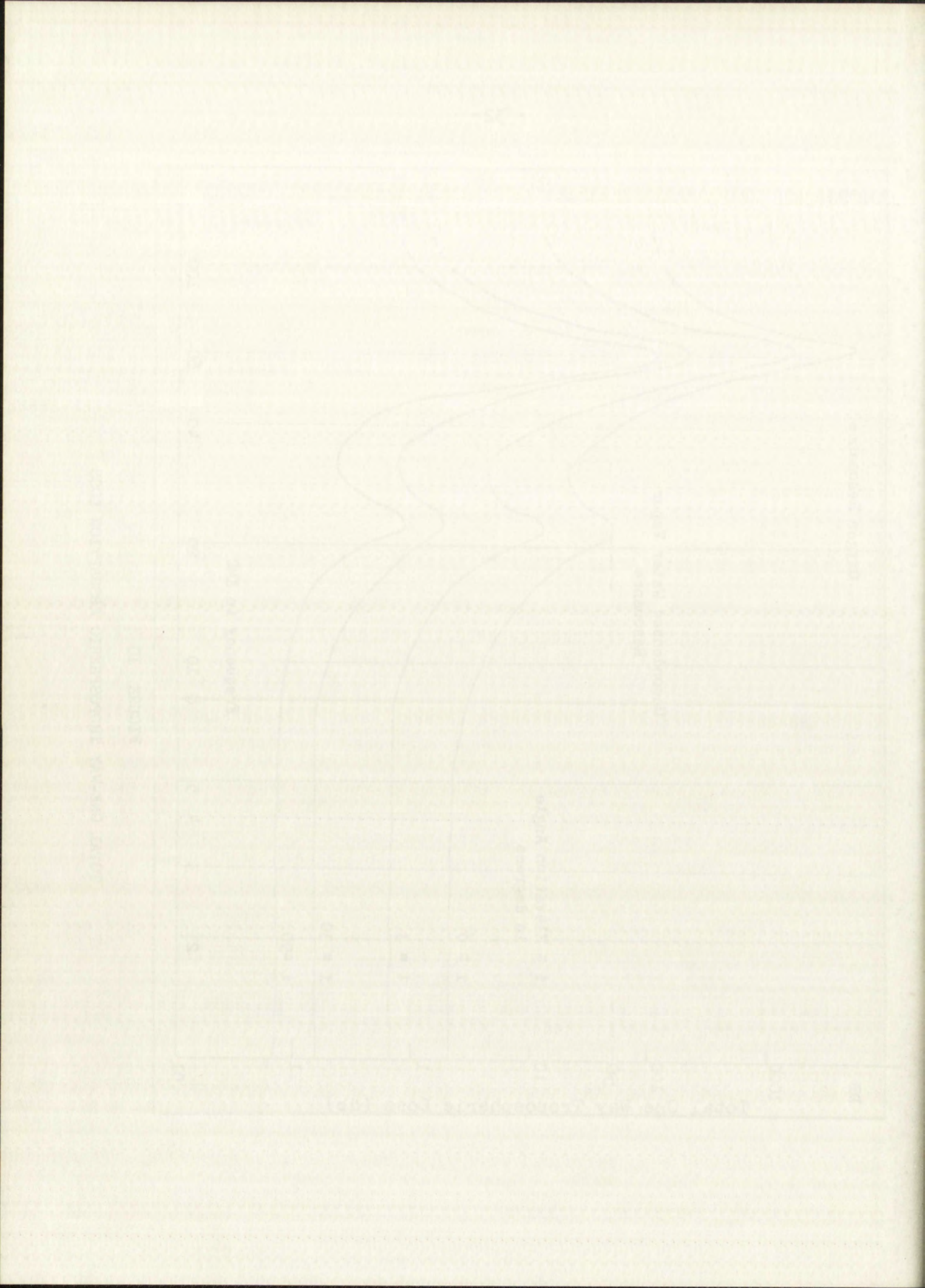

CHAPTER III

THE APPLICATION OF INFORMATION THEORY TO RADAR ACCURACY

Inherent Radar Accuracy

We will now proceed to analyze mathematically the information content of our received radar signal with the purpose of specifying the factors that influence the inherent radar accuracy. The material presented is an application of the basic literature on the estimation of signal parameters in the presence of noise[12-16], with the notation of Woodward being followed in general.

---

12. D. Slepian, "Estimation of Signal Parameters in the Presence of Noise", IRE Trans. on Information Theory, Vol. IT-3, pp 68-89, March, 1954.

13. V.A. Kotel'nikov, "The Theory of Optimum Noise Immunity" McGraw-Hill Book Co., Inc., New York, Chap. 6, 1959.

14. P.M. Woodward, "Probability and Information Theory with Applications to Radar", McGraw-Hill Book Co., Inc., New York, 1953.

15. A. J. Mallinckrodt and T.E. Sollenberger, "Optimum Pulsetime Determination", IRE Trans. on Information Theory, Vol. IT-3, pp 151-159, March, 1959.

16. W. McSiebret, "A Radar Detection Philosophy", IRE Trans. on Information Theory, Vol. IT-2, pp 204-221 September, 1956.

We will be concerned more with the determination of the effects of atmospheric noise on signal parameters than with the statistical problem of the minimum detectable signal and the maximum range[17].

At our radar receiver we will receive a signal which is a mixture of noise and the actual target return. It will be the job of our receiver to sort the information in this signal and present to us the best possible picture of the target return signal information. The transmitted signal, the noise, and the received signal will all have certain probability distributions associated with them. We are interested in the gain in information after having received this combined return signal. After Shannon and Weaver[18] the information content of a message state of probability P is -log P. If we define I = Information Gain = Initial Information - Final Information, we get

$$I_{xy} = [-\log P(x)] - [-\log P_y(x)] = \log\left[P_y(x)/P(x)\right] \quad (16)$$

where P(x) is the probability of message state x prior to receiving the communication, i.e. the prior probability, and $P_y(x)$ is the probability of message state x given the

---

17. J. Marcum and P.Swerling, "Studies of Target Detection by Pulsed Radar", IRE Trans. on Information Theory, Vol. IT-6, No. 2, April 1960.

18. C.E.Shannon and W.Weaver, "The Mathematical Theory of Communication", University of Illinois Press, Urbana, Illinois, 1949.

communication y. This definition of information gain agrees with intuitive ideas of information in that receiving a signal concerning an event of high probability gives only a small amount of information while receipt of a signal indicating an unlikely event is more significant. Our definition of Information Gain will be positive when $P_y(x)$ is greater than $P(x)$. $P_y(x)$ can be either greater or less than $P(x)$ and in the case where x and y are independent, I will be zero, and there is no information transfer.

It has been shown[17] that an optimum receiver can never extract more information than that contained in $P_y(x)$. Our attention will be directed at the evaluation of this conditional probability function. $P_y(x)$ is often referred to as the "inverse probability", the "inverse" resulting from the fact that we are using the effect y, to specify the cause x. A simple example is given that will introduce the method of determination of the inverse probability. This will lead into the development of $P_y(x)$ for x, a radar signal in the presence of noise.

Example of the Inverse Probability Using Discrete Variables

Using a group of dice 1/4 of which are good (regular) and 3/4 of which have two blank sides (bad), we roll one and observe the output, y, i.e. the side of the die that lands face upwards. The message state we are interested in is

Whether the die is good or bad. From the observed effect y, the best our mental receiver can do for us would be to establish the "inverse probability" as to whether the die is good or bad. From the product law of probability

$$P(y)P_y(x) = P(x)P_x(y)$$

or

$$P_y(x) = \frac{P(x)P_x(y)}{P(y)} \tag{17}$$

where $P_y(x)$ is the inverse probability we are looking for. For our example there are only two message states possible, x_1 that we have a good die, and x_2 that we have a bad one. There are also only two results possible, y_1 that we observe a numbered side and y_2 that we observe a blank side. In line with our previous notation $P_{y1}(x_2)$ would be the probability that the die would be bad, given that we have observed a numbered side thrown, with

x_1, good	$P(x_1) = 1/4$
x_2, bad	$P(x_2) = 3/4$
y_1, numbered side	$P_{x1}(y_1) = 1$
y_2, blank side	$P_{x1}(y_2) = 0$
	$P_{x2}(y_1) = 2/3$
	$P_{x2}(y_2) = 1/3$

Starting with our observation we assume we have observed a blank side, then

$$P_{y2}(x_1) = \frac{P(x_1)\, P_{x1}(y_2)}{P(y_2)} \qquad (18)$$

$$P_{y2}(x_2) = \frac{P(x_2)\, P_{x2}(y_2)}{P(y_2)}$$

Inserting the appropriate values

$$P_{y2}(x_1) = (1/4)\,\frac{0}{P(y_2)} = 0$$

and since $P_{y2}(x_1) + P_{y2}(x_2) = 1$

$$P_{y2}(x_2) = 1$$

This is of course intuitively obvious since once a blank side is observed we know that we have a bad die.

In the case where the observed result is y_1, a numbered side

$$P_{y1}(x_1) = \frac{1/4 \cdot 1}{P(y_1)} = \frac{1}{4P(y_1)}$$

$$P_{y1}(x_2) = \frac{(3/4)\,(2/3)}{P(y_1)} = \frac{1}{2P(y_1)}$$

since

$$P_{y1}(x_1) + P_{y1}(x_2) = 1$$

$$\frac{1}{4P(y_1)} + \frac{1}{2P(y_1)} = 1$$

therefore

$$P(y_1) = 3/4$$

and

$$P_{y1}(x_1) = 1/3$$

$$P_{y1}(x_2) = 2/3$$

Therefore the probability that the die is good is 1/3 and the probability that it is bad is 2/3. This is the best description of the die possible with the information on hand. We might continue to throw this die since we are still not sure of its message state. To continue correctly we would take advantage of the previous information and use 1/3 and 2/3 as our prior probabilities rather than 1/4 and 3/4 which were our original prior probabilities. If we were to continue we would have a new set of prior probabilities dependent on the information discovered from the previous throw. This is somewhat analagous to the multiple returns we receive from a radar target and place on the scope, as each return is swept across on top of the others combining the information to give us a better idea of the signal.

Signals in Gaussian Noise

Making use of this idea of inverse probability we look at a case that is closer to an actual radar signal. We look at an output, y, composed of an input signal u_x, a steady voltage lasting for a time T, and a superimposed random white Gaussian noise voltage n(t). Gaussian noise is described by the Gaussian or normal distribution and is distributed about a mean of zero, with some mean squared value N. With

$$y = u_x + n(t) \tag{19}$$

the distribution of y will be Gaussian about the signal value u, and therefore the conditional probability density function can be written

$$P_x(y) = \frac{1}{\sqrt{2\pi N}} \exp\left[-\frac{(y-u_x)^2}{2N} \right] \qquad (20)$$

If the signal value were zero then we would have y simply composed of the noise with

$$P_x(y)\Big|_{u=0} = \frac{1}{\sqrt{2\pi N}} \exp\left[\frac{-y^2}{2N} \right] \qquad (21)$$

We would be interested in the inverse probability which would be

$$P_y(x) = \frac{p(x)}{p(y)} \cdot p_x(y)$$

or

$$P_y(x) = C\, p(x) \exp\left[\frac{-(y-u_x)^2}{2N} \right] \qquad (22)$$

where

$$C = \frac{1}{p(y)\sqrt{2\pi N}}$$

In order to extract all the information in y(t) it is not necessary to observe it continuously but only to sample it at certain intervals. To justify this we must make use of the "Sampling Theorem" of waveform analysis. This theorem says in essence that given a function y(t) containing no frequencies higher than B cycles per second, the function is completely determined by giving its ordinates at a series

of points spaced no more $\frac{1}{2B}$ seconds apart, the series extending throughout the time domain. In using the sampling theorem we assume that the noise contains no frequencies greater than B, where B is chosen arbitrarily large and is greater than $\frac{1}{T}$ the interval of the signal u_x. These assumptions are adequate for dealing with a practical detected signal. For a radio frequency signal B would have to be greater than the carrier frequency plus the side band frequency spread. White Gaussian noise is a reasonable model for physical noise and can be described as follows. The probability functions on the noise samples are Gaussian. The power spectrum of the noise is flat over the bandwidth considered. It is then apparent that the total noise power N is proportional to the bandwidth B, with

$$N = BN_o \tag{23}$$

where N_o is the noise power per unit bandwidth. A very useful property of bandwidth limited white noise is that the samples, n_j, taken at intervals of $\frac{1}{2B}$ are statistically independent. This property simplifies much of the following work.

The complete characteristics of our inverse probability will be determined by our j samples. Since the first y value observed will influence the prior probability for the second we have a situation akin to that of repeatedly throwing the same die. The $p_y(x)$ for the first example

becoming the prior probability for the second. With $p_m(x)$ as the conditional probability density after m samples

$$p_m(x) = k \prod_{j=1}^{j=m} p_o(x) p_x(y_j) \tag{24}$$

for our example then

$$p_{y_j}(x) = k_j \, p_o(x) \exp \left[\frac{-(y_j - u_x)^2}{2N} \right] \tag{25}$$

and therefore

$$p_y(x) = k \, p_o(x) \prod_{j=1}^{j=m} \exp \frac{-(y_j - u_x)^2}{2N} \tag{26}$$

$$= k \, p_o(x) \exp \sum_{j=1}^{j=m} \frac{(y_j - u_x)^2}{2N} \tag{27}$$

Using the development from the sampling theorem for the relationship between a squared sample sum and the integral of the squared continuous time function we get

$$p_y(x) = k \, p_o(x) \exp \left[-2B \int_{-\infty}^{\infty} \frac{(y-u_x)^2}{2N} \, dt \right] \tag{28}$$

$$= k \, p_o(x) \exp \left[-\frac{1}{N_o} \int_{o}^{T} (y-u_x)^2 dt \right] \tag{29}$$

This equation applies to all problems of reception in the presence of white Gaussian noise, in the absence of stray parameters.

To review then we have examined a constant signal lasting for a time T, the output y(t) being a mixture of white Gaussian noise and this input signal. We have de-

termined the inverse probability function which tells us as much as we can possibly know about the input signal, given the function y(t).

For our simulated radar signal the u_x will itself be time dependent as well as the added white Gaussian noise.

$$y(t) = u_x(t) + n(t)$$

and again

$$p_y(x) = k\, p(x) \exp\left[-\frac{1}{N_o}\int_0^T (y-u_x)^2 dt\right]$$

with the exception that now u_x is a function of t.

Measurement of Time Delay

To simulate an actual radar signal, we will assume exactly the same criteria with the exception that our signal $u_x(t)$ will suffer a delay of τ between transmission and reception. Due to the convenience of the mathematics, we will use the complex signals $\gamma(t)$, $\Psi(t)$, $\nu(t)$, with $\gamma(t)$ our received signal, $\Psi(t)$ our transmitted signal, and $\nu(t)$ the white Gaussian noise. Since the complex signals will represent real signals, certain restrictions are imposed on the complex signals. Gabor[19] has described the analytical generation of a complex function $\Psi(t)$ corresponding to a real function u(t). For a real u(t) limited to a certain finite T, the energy of the signal has a finite value E,

---

19. D.Garbor, Journal of the Institute of Electrical Engineers, part IV, No. 93, pp 429, 1946.

$$E = \int_{-\infty}^{\infty} u(t)^2 \, dt \tag{30}$$

If u(t) is periodic, the infinite integral fails to converge. The limits may then be taken over a finite integral number of periods, with E representing the energy of the signal between the limits. E can also be expressed as the integral of the energy density curve.

$$E = \int_{-\infty}^{\infty} \left|F(f)\right|^2 \, df \tag{31}$$

where F(f) is the Fourier transform of f(t)

$$F(f) = \int_{-\infty}^{\infty} f(t) \exp(-2\pi jft) \, dt \tag{32}$$

since for a real f(t), $\left|F(f)\right|$ is an even function

$$E = \int_0^{\infty} 2 \left|F(f)\right|^2 \, df = \int_0^{\infty} \mathcal{E}(f) \, df \tag{33}$$

where $\mathcal{E}(f) = 2\left|F(f)\right|^2$ the energy spectral density. A complex waveform, equivalent to our real f(t) is then specified by the energy spectral density between 0 and ∞. If the frequency range is restricted to between 0 and f

$$E = \int_0^{f} 2 \left|F(f)\right|^2 \, df \tag{34}$$

and the energy spectral components determine our equivalent $\gamma(t)$.

Our waveform which is transmitted, reflected, returned and received after suffering a delay τ_0 is

$$\gamma(t) = \Psi(t-\tau_0) + \nu(t) \tag{35}$$

This is an extremely simplified expression for an actual radar signal. The target has been assumed stationary in which case τ_0 is not a function of time. No account of any change of wave shape or amplitude has been made. There will be no change in wave shape during propagation through the atmosphere when the index is independent of frequency. Each spectral component will travel at the same speed through media of constant index and the combination of these components will continue to form the original wave shape. The effect on the wave when the index becomes frequency sensitive will be covered in Chapter V. While in the case of a radar return signal from a radar beacon, the amplitude might be known, generally this will not be true. Also the reflection characteristics of the target may alter the wave shape. Neglecting any change in wave shape, in practice our inverse probability will be a function of the time as well as the stray parameter amplitude. We have our choice of destroying the amplitude information by integration over all values of amplitude or presenting this redundant and unwanted information. While our inverse probability would be effected by the amplitude probability, all the time information available can be determined from the comparison of the received signal and a scaled version of the transmitted signal[20]. To summarize our assumptions then we have

---

20. P. M. Woodward, Op Cit. pp 94-95.

for simplicity no stray amplitude parameter, and τ is independent of time. If we can express the inverse probability, $p_\gamma(\tau)$, the probability of the time lag, given some signal $\gamma(t)$, we will have the best description of the time lag.

$\gamma(t)$, $\Psi(t)$ and $\nu(t)$ will all be typical high frequency functions and the advantage of the complex notation is that we can define appropriate low frequency functions,

$$\begin{aligned} \gamma(t) &= y(t) \exp(j2\pi f_o t) \\ \Psi(t) &= u(t) \exp(j2\pi f_o t) \\ \nu(t) &= n(t) \exp(j2\pi f_o t) \end{aligned} \tag{34}$$

where the signal is limited to some total time T.

The inverse probability with respect to τ can be written

$$p_\gamma(\tau) = K\, p(\tau) \exp - \frac{1}{2N_o} \int_0^T \left|\gamma(t) - \Psi(t-\tau)\right|^2 dt \tag{35}$$

Here the appropriate complex terms have been inserted and τ or $t-\tau$ has been used as a parameter where applicable. This equation has the same form as (29) and is its counterpart applying like (29) to all problems of reception in the presence of white Gaussian noise, in the absence of stray parameters[21]. Expanding the integrand we get

$$p_\gamma(\tau) = Kp(\tau)\exp\left[\frac{-1}{2N_o} \int_0^T \left(\left|\gamma(t)\right|^2 + \Psi(t-\tau)^2 - 2R\left\{\gamma^*(t)\Psi(t-\tau)\right\}\right)dt\right] \tag{36}$$

---

21. P.M. Woodward, Op Cit., pp 79-80.

where $R\{x\}$ indicates taking the real part of x. The input to our receiver $\gamma(t)$ will be observed over some period T, which we will insure is large enough to include all values of τ. The first term in the integrand is not a function of τ, if as we have assumed, the period of observation T is large enough to include all possible values of τ. For this reason we can include it in our normalizing constant K. Similarly

$$\int_0^T \left|\Psi(t-\tau)\right|^2 dt \tag{37}$$

is the received signal energy and will be independent of τ if T is large enough and $\Psi(t)$ finite in duration. The inverse probability then simplifies to

$$p_\gamma(\tau) = K\, p(\tau)\, \exp\left[\, R\left\{\frac{1}{N_o}\int_0^T \gamma^*(t)\, \Psi(t-\tau)\right\} dt \,\right] \tag{38}$$

Now expressing our probability in terms of the low frequency functions

$$p_y(\tau) = Kp(\tau)\exp\left[\, R\left\{\frac{1}{N_o}\int_0^T y^* e^{-2\pi j f_o t} u(t-\tau) e^{2\pi j f_o (t-\tau)} dt\right\}\right] \tag{39}$$

$$= Kp(\tau)\exp\left[\, R\left\{\frac{1}{N_o}\, e^{2\pi j f_o \tau} \int_0^T y^*(t) u(t-\tau)\, dt\right\}\right] \tag{40}$$

This is our complete inverse probability. The informationally important operation is the convolution of $y(t)$ and $u(-t)$. The rest of the information in the inverse probability can be supplied without reference to $y(t)$. Because these operations are reversible they are informationally insignificant. The only informationally significant operation takes place in the integration of $y^*(t)u(t-\tau)$.

The factor $e^{-2\pi j f_o \tau}$ represents the high frequency phase information. Due to its ambiguity, this information is useless to us. We are interested in the low frequency waveforms. The proper method of taking advantage of the low frequency information is to "smooth" $p_y(\tau)$.

This does not give us precisely the upper envelope, but a trace similar to it where the area under each radio frequency cycle is preserved. Letting

$$q = e^{-2\pi j f_o} \frac{1}{N_o} \int_0^T y^*(t)u(t-\tau)\, dt \qquad (41)$$

we can express q as the combination of envelope and high frequency function where

$$R\{q\} = R\left\{e^{-2\pi j f_o} \frac{1}{N_o} \int_0^T y^*(t)u(t-\tau)\, dt \right. \qquad (42)$$

$$= R\left\{|q| \underline{\angle \theta + 2\pi f_o \tau}\right\}$$

$$= |q| \cos(2\pi f_o \tau + \theta)$$

Our smoothing requires that we preserve the area as follows

$p_y(\tau)$ = the smoothed probability

$$P_y(\tau) = K\, p_y(\tau) \int_{\tau - \frac{\pi}{\omega_o}}^{\tau + \frac{\pi}{\omega_o}} \exp \left[q \cos (2\pi f_o \tau + \theta) \right] d\tau \quad (42)$$

This is the integral expression for the modified Bessel Function I_o with the argument q, where the assumption has been made that the variation of q and θ is negligible between the limits. The modified Bessel function is a Bessel function of the first kind but having an imaginary argument.

$$I_o(|q|) = J_o\left[(-1)^{1/2}|q|\right] = \frac{e^{|q|}}{(2\pi q)^{1/2}}\left(1 + \frac{1}{8q} + \ldots\right) \quad (43)$$

A graph of $I_o(|q|)$ is shown in Figure 11. Our inverse probability is then

$$P_y(\tau) = K\, p(\tau)\, I_o(|q|) \quad (44)$$

Time Measurement Accuracy

In order to specify the accuracy of time measurement we will analyze the characteristics of $P_y(\tau)$ in the vicinity of the true value of time lag τ_o. As a mathematical convenience we split y(t) into signal and

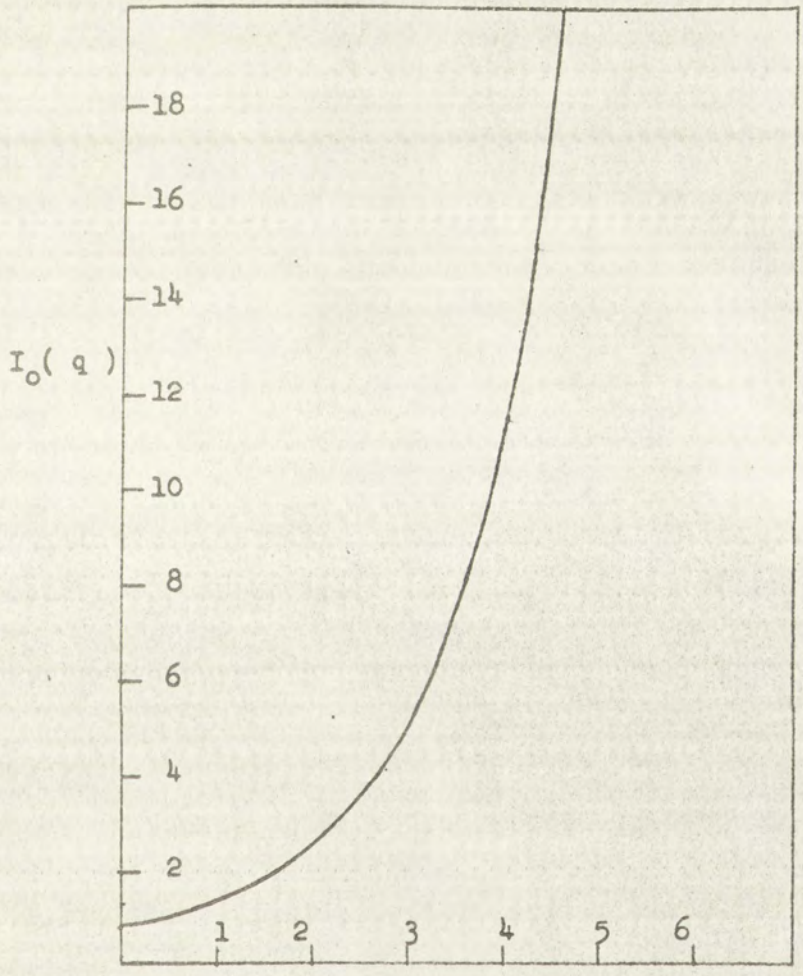

FIGURE 11

MODIFIED BESSEL FUNCTION

noise components

$$Y(t)\, e^{2\pi j f_o t} = u(t-\tau_o) e^{2\pi j f_o t} e^{-2\pi f_o \tau_o} + n(t) e^{2\pi j f_o t} \tag{45}$$

$$Y(t) = u(t-\tau_o) e^{-2\pi j f_o \tau_o} + n(t)$$

Expanding $|q|$ into the low frequency noise and signal contributions

$$q = |g + h| \tag{46}$$

$$= \left| \frac{1}{N_o} \int_0^T y^*(t)\, u(t-\tau)\, dt \right|$$

$$= \left| \frac{1}{N_o} \int_0^T u^*(t-\tau_o) u(t-\tau)\, dt \right.$$

$$\left. + \frac{1}{N_o} \int_0^T n^*(t) u(t-\tau) e^{2\pi j f_o \tau_o}\, dt \right| \tag{47}$$

$g(\tau)$ then is the contribution due to signal and $h(\tau)$ is the contribution due to the noise. These expressions are familiar as the signal autocorrelation and the signal and noise cross correlation functions. Then

$$P_y(\tau) = k\, p(\tau)\; I_o |(g + h)| \tag{48}$$

We have assumed $\frac{2E}{N_o}$ is much greater than one, and an immediate consequence of this is that the peak of the signal function $g(\tau)$ will be large compared with unity and will

occur at τ_o. This will be accentuated in the inverse probability distribution since $I_o(x)$ asymptotically approaches an exponential behavior for large x. Except near this peak the signal function $g(\tau)$ will have little effect on $P_y(\tau)$. While $g(\tau)$ will always have a peak or maximum at τ_o, the inclusion in $q(\tau)$ of $h(\tau)$, the noise component, will randomly displace this peak from the mean value at τ_o. If we consider the contribution of $g(\tau)$ to the inverse probability in the vicinity of τ_o we can expand $g(\tau)$ around τ_o making use of Taylor's expansion where

$$g(\tau_o) = \frac{1}{N_o}\int_0^T u^*(t-\tau_o)u(t-\tau_o)\,dt \qquad (49)$$

This integral is simply the energy of our complex transmitted signal, 2E, and therefore

$$g(\tau_o) = \frac{2E}{N_o} \qquad (50)$$

Taylor's theorem states that

$$f(x) = f(a) + f'(a)(x-a) + \frac{f''(a)(x-a)^2}{2!} + \cdots \qquad (51)$$

The values of $g'(\tau_o)$ and $g''(\tau_o)$ must be determined. Since for practical radar signals the peak around τ_o will be quite sharp we will ignore powers of $(\tau - \tau_o)$ greater than the second.

$$g'(\tau_o) = \frac{1}{N_o} \int_0^T u^*(t-\tau_o)\, u'(t-\tau_o)\, dt \qquad (52)$$

$$g''(\tau_o) = \frac{1}{N_o} \int_0^T u^*(t-\tau_o)\, u''(t-\tau_o)\, dt \qquad (53)$$

Through the use of the generating function for the moments of the energy spectrum[22] we can relate these equations to their Fourier transforms. The basic equation is

$$\int_{-\infty}^{+\infty} \Psi^* \frac{d^n}{dt^n} (\Psi)\, dt = (2\pi j)^n \int_{-\infty}^{+\infty} \Phi^* f^n \Phi\, df \qquad (54)$$

where $\Phi(f)$ is the Fourier transform of $\Psi(t)$. This relationship can be derived from Parseval's Theorem and repeated application of the rule for the transform of a derivative. This was in fact the mathematical basis for our definition of the carrier frequency f_o.

$$\int_{-\infty}^{+\infty} \Psi^* \Psi'\, dt = 2\pi j \int_{-\infty}^{\infty} \Phi f \Phi df = 4\pi j\, E\, f_o \qquad (55)$$

---

22. D. Gabor, op cit.

Substituting $u(t)\, e^{2\pi j f_o t} = \Psi(t)$ into the moment generating function after a little manipulation we get

$$\int u\, u'\, dt = 2\pi j \int U\, f\, U\, df = 0 \qquad (56)$$

where U(f) is the Fourier transform of u(t). This relationship simply demonstrates that the carrier frequency has been defined as the spectral centroid of U(f). The normalized second moment of U(f) is defined as U_2.

$$U_2 = \left(\frac{\beta}{2\pi}\right)^2$$

$$\beta^2 = (2\pi)^2\, U_2 \qquad (57)$$

where β is then defined as our effective bandwidth or more formally β is twice the root mean square deviation of the energy spectrum with respect to the carrier frequency. β is important as we will use it as the significant parameter describing the frequency spectrum of our signal.

$$\beta^2 = \frac{(2\pi)^2 \int U^*\, f^2\, U\, df}{\int U^*\, U\, df} \qquad (58)$$

or

$$\int u^*\, u''\, dt = -2E\beta^2 \qquad (59)$$

Making use of the values of $g(\tau_o)$, $g'(\tau_o)$ and $g''(\tau_o)$ in the

Taylor's expansion

$$g(\tau) = \frac{2E}{N_o} + 0 + \left[-\frac{1}{2}\frac{2E}{N_o}\beta^2\right](\tau - \tau_o)^2 \qquad (60)$$

In the vicinity of τ_o the high value of $g(\tau)$, due to the signal, makes the significant contribution to $P_y(\tau)$. Looking at our inverse probability in the vicinity of τ_o and considering only the contribution of $g(\tau)$

$$P_y(\tau) = k\, p(\tau)\, I_o(|g|) \qquad (61)$$

For this high value of $g(\tau)$, $I_o(|g|)$ as can be seen from Figure 11 will be exponential. $P_y(\tau)$ then equals

$$P_y(\tau) = k\, p(\tau) \exp\left(\frac{2E}{N_o}\right) \exp\left[\frac{-\frac{1}{2}(\tau-\tau_o)^2}{\frac{N_o}{2E\beta^2}}\right] \qquad (62)$$

$P_y(\tau)$ is then Gaussian in the vicinity of τ_o if $p(\tau)$ is varying slowly or is constant in this area. This is a reasonable assumption and in that case the accuracy with which τ_o can be determined has a standard deviation

$$\delta_\tau = \frac{1}{\beta\left[\frac{2E}{N_o}\right]^{\frac{1}{2}}} \qquad (63)$$

Actually if the only contribution to $P_y(\tau)$ in the vicinity of τ_o were $g(\tau)$ we could take the peak of our inverse probability distribution which would occur exactly at τ_o and τ_o would then be completely determined. The inclusion of $h(\tau)$, which is a random function with both real and imaginary parts being Gaussian and having a mean of zero, will not effect the spread of $P_y(\tau)$ but only shift the peak from τ_o to some value τ_m in the vicinity of τ_o. The distribution is then

$$P_y(\tau) \propto \exp\left[-\frac{1}{2}\,\frac{(\tau-\tau_m)^2}{\frac{N_o}{2E\beta^2}}\right] \qquad (64)$$

and the accuracy of measurement of τ is still given by the same standard deviation. A rigorous derivation of the effect of including $h(\tau)$ in the vicinity of τ_o is given by Woodward and Davies [23] giving the above result.

For a large signal to noise ratio the accuracy of measurement is then inversely proportional to

$$\beta\left[\frac{2E}{N_o}\right]^{\frac{1}{2}}$$

When the medium external to the radar contributes any substantial increase in the noise, we decrease our signal to

---

23. P.M. Woodward and I.L. Davies, "The Theory of Radar Accuracy", Philosophical Magazine No. 41 pp 1001, Nov. 1950.

noise ratio and our range accuracy falls off. Obtaining only these minimum errors is based on the use of a receiver that will take advantage of the information available in our radar signal by performing the necessary cross correlation. This in itself depends on the comparison of a copy of the original signal and the reflected signal. Any significant change in the original signal wave shape will invalidate the basis for our determination of the time measurement accuracy. In any situation then where ray theory is not applicable our analysis is suspect.

Summing up the results of the analysis we see that we can relate the standard deviation in time measurement to range accuracy where

$$\delta_r = \frac{c}{2}\,\delta_\tau = \frac{c}{2} \cdot \frac{1}{\left[\frac{2E}{N_o}\right]^{\frac{1}{2}}} \tag{65}$$

This then is the significant result of this chapter. We have assumed a propagation velocity equal to c the speed of light. For pulsed radar then a simple maximization of the signal to noise ratio will not alone guarantee a maximization of range accuracy.

CHAPTER IV

APPLICATION OF RADAR PULSE ANALYSIS TO DETERMINATION OF RANGE ACCURACY

Accuracy of Rectangular Pulses

Having determined the theoretical radar range accuracy of our equipment we now compare the use of different types of pulses. It is apparent that the β figuring in our accuracy expression will be different for different types of pulses. Since β is twice the root mean square deviation of the energy spectrum with respect to the carrier frequency, we will be concerned with developing the Fourier transforms of the pulses to be compared.

The standard periodic rectangular pulse is briefly considered as an introduction, realizing that while perfect rectangular pulses are not obtainable they can be closely approximated in practice.

Using Fourier series to analyze the waveshape of Figure 12

$$f(t) = \frac{1}{T_2} \sum_{-\infty}^{\infty} C_n \quad e^{j\omega_n t} \tag{65}$$

$$C_n = \int_{\frac{-T_1}{2}}^{\frac{T_1}{2}} f(t)\, e^{-j\omega_n t} \, dt \tag{66}$$

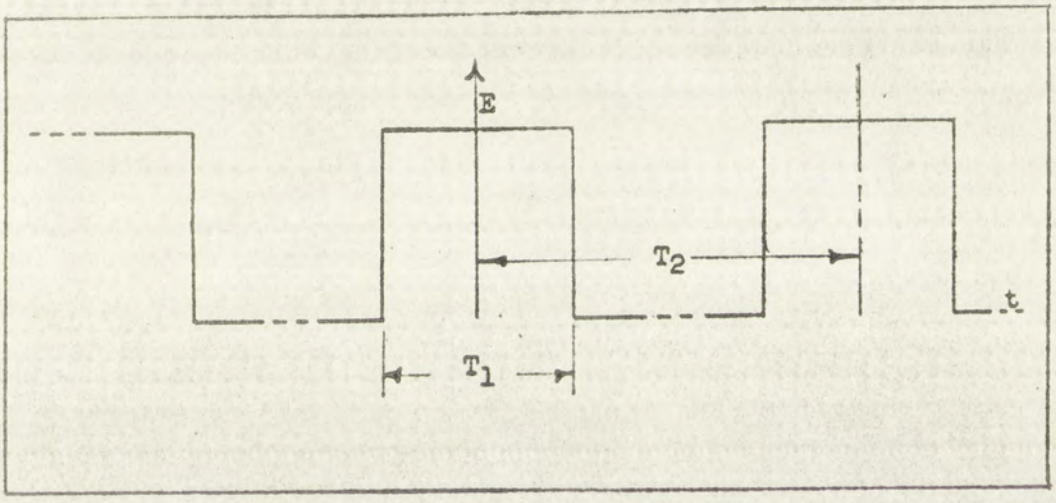

FIGURE 12

PERIODIC RECTANGULAR WAVE

(ENVELOPE OF RADIO FREQUENCY SIGNAL)

$$C_n = \int_{-\frac{T_1}{2}}^{\frac{T_1}{2}} E\, e^{-j\omega_n t}\, dt = E \left[\frac{e^{j\omega_n \frac{T_1}{2}} - e^{-j\omega_n \frac{T_1}{2}}}{j\omega_n} \right] \quad (67)$$

$$C_n = E\, T_1 \, \frac{\sin \frac{\omega_n T_1}{2}}{\frac{\omega_n T_1}{2}} \quad (68)$$

Since we have a periodic wave, ω_n is discrete,

$$\omega_n = 2\pi f_n = 2\pi n \frac{1}{T_2}$$

where n is any integer. The spacing between the harmonic components is therefore $\frac{1}{T_2}$. The amplitude of the frequency spectrum will equal zero where

$$\sin \frac{\omega T_1}{2} = 0, \quad \text{or} \quad f = \frac{n}{T_1} \quad (69)$$

Our assumed radar signal will be composed of a sinusoidal carrier frequency, the envelope of which will give us the low frequency signal described. Multiplying the low frequency envelope by $\cos(\omega_o t)$ gives us for our high frequency radar pulse

$$f(t) = \frac{\cos(\omega_o t)}{T_2} \sum_{n=-\infty}^{n=\infty} C_n\, e^{j\omega_n t} \quad (70)$$

$$f(t) = \frac{ET_1}{T_2} \cos\omega_o t \quad \frac{\sin\frac{\omega_n T_1}{2}}{\frac{\omega_n T_1}{2}} \quad e^{j\omega_n t} \qquad (71)$$

Figure 13 is a graph of the spectrum of the periodic pulse. If we had considered a single pulse (non-periodic) with the same parameters, the difference in the results would have been a continuous energy density rather than discrete energy spectrum.

For radar signals T_1 is usually much smaller than T_2. Since the first crossing of the axis occurs at $f_o \pm \frac{1}{T_1}$ we can see that as the pulse width or duration is increased the frequency spread between f_o and the axis crossing decreases. This indicates an inverse relationship between the bandwidth and pulsewidth. Most of the energy of the pulse will be contained in the harmonic components lying in the band $f_o \pm \frac{1}{T_1}$.

Since perfect rectangular pulses requiring an infinite bandwidth cannot be realized we will be concerned with the appropriate choice of a bandwidth around the carrier frequency. Limiting the bandwidth will in turn lead to a non zero rise and fall time for the edges of the pulse. The greater the bandwidth the more precise is the presentation of the wave. Unfortunately the noise energy is proportional to the bandwidth, and the greater.

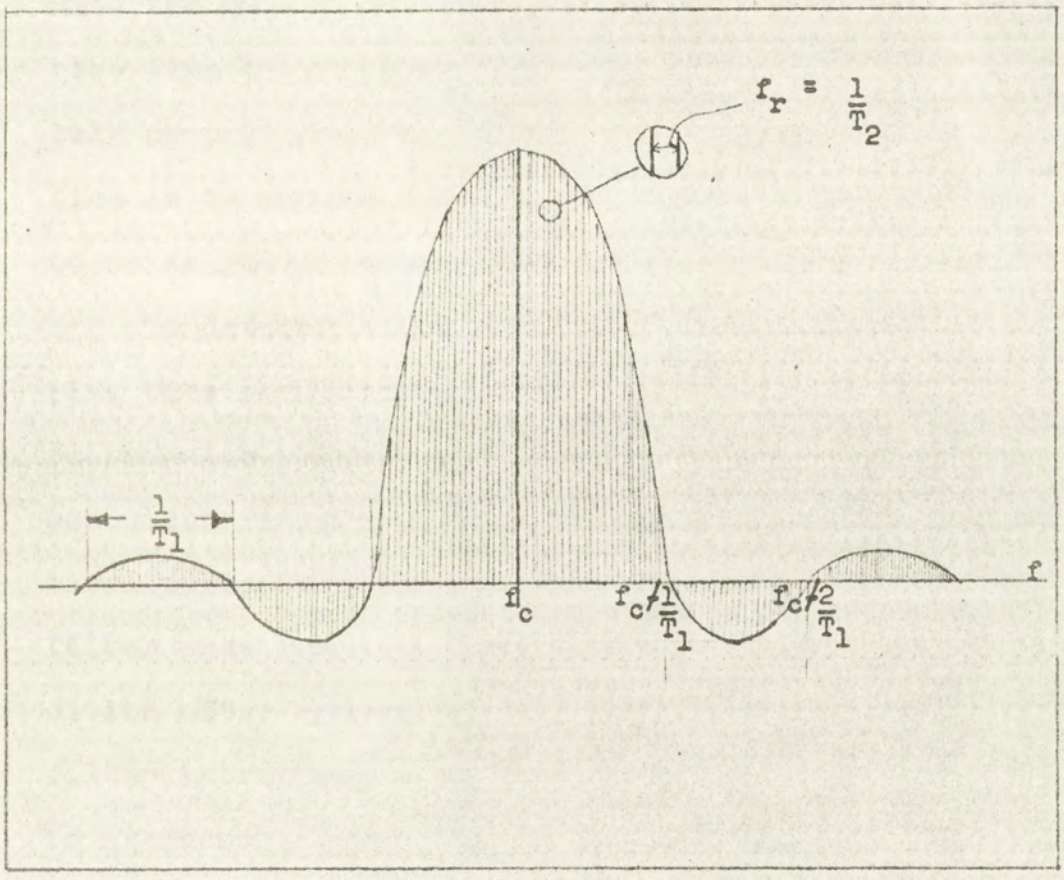

FIGURE 13

SPECTRUM OF PERIODIC RECTANGULAR WAVE

the bandwidth, the greater the RMS noise voltage. From Figure 14 we can approximately maximize the signal to noise level by choosing a value of bandwidth B in the range of $\frac{1}{2T_1}$ to $\frac{2}{2T_1}$. Choosing a value of bandwidth in this range will not necessarily maximize our accuracy. Most practical high accuracy radars concern themselves with the detection of the leading edge of a pulse. The rise time of an approximately rectangular pulse is inversely proportional to the bandwidth. The general practice is to expand the bandwidth at some loss in signal to noise ratio in order to get sharper leading edges.

To determine the approximate relations between rise time and bandwidth, let us consider a "practical" rectangular pulse. To simulate a practical pulse we bandwidth limit a perfectly rectangular wave. Our practical pulse then is the output from a perfect bandpass filter when the input is a rectangular pulse. As a condition often encountered in practice we will assume the filter introduces a phase shift linearly proportional to frequency, equal to - $g\omega$.

Using the complex notation with Y(t) out output and $e^{-j\omega g}$ the transform describing our filter

$$Y(t) = \frac{1}{2\pi} \int_{-\omega_s}^{+\omega_s} e^{-j\omega g} \frac{(e^{-j\omega T_1} - 1)\, e^{j\omega t}}{-j\omega} \, d\omega \qquad (72)$$

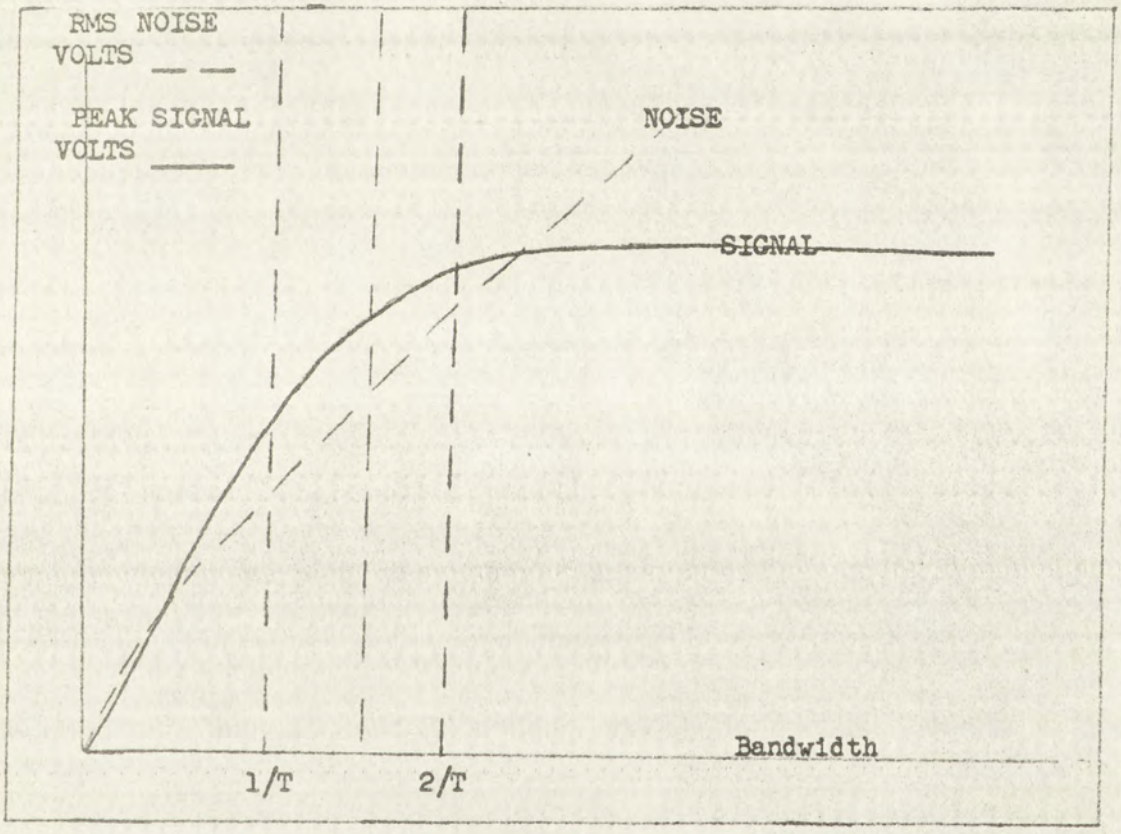

FIGURE 14

ILLUSTRATION OF NOISE VOLTAGE AND SIGNAL VOLTAGE VARIATION WITH I.F. BANDWIDTH

where we are analyzing only the low frequency envelope and

$$2\omega_s = 2\pi B \tag{73}$$

$$Y(t) = \frac{1}{2\pi}\int_{-\omega_s}^{\omega_s} \frac{j}{\omega}\left(e^{j\omega(t-g-T_1)} - e^{j\omega(t-g)}\right) d\omega \tag{74}$$

letting $m = \omega(t-g)$ and $v = \omega(t-g-T_1)$

$$Y(t) = \frac{1}{\pi}\int_0^{\omega_s(t-g)} \frac{\sin m}{m}\, dm - \int_0^{\omega_s(t-g-T_1)} \frac{\sin v}{v}\, dv \tag{75}$$

$$Si(x) = \int_0^x \frac{\sin x}{x}\, dx$$

therefore

$$Y(t) = \frac{1}{\pi}\left[Si(\omega_s[t-g]) - Si(\omega_s\,[t-g-T_1])\right] \tag{76}$$

where Si(x) can be expanded in a power series. Tables are available for the value of the integral given x. Figure 15 is a graph of Si(x). For x less than -1.92 Si(x) approximates $-\frac{\pi}{2}$. For x greater than 1.92 Si(x) approximates $\frac{\pi}{2}$. Around zero the Si(x) rises from $-\frac{\pi}{2}$ at x = -1.92 to a value of $\frac{\pi}{2}$ at x = 1.92. There is a slight overshoot with the value of Si(3.14) = .54. Figure 15 shows the output of our low pass filter. If our pulse is wide enough so that the rise and fall times

do not overlap, the contribution from the second term in Y(t) will approximately be $\frac{\pi}{2}$ and

$$Y(t) = \frac{1}{\pi}\left[Si(\omega_s[t-g]) + \frac{\pi}{2}\right] \tag{77}$$

From Figure 15 then our pulse will rise from 0 to 1.09 in the time from $\frac{g - 1.92}{\omega_s}$ to $\frac{g + 3.14}{\omega_s}$. The rise time is then

$$t_r = \frac{5.06}{\omega_s} = \frac{.805}{f_s} \tag{78}$$

For a high frequency radar pulse of carrier frequency f_o and a bandwidth B, the rise time equals $\frac{1.61}{B}$ and the time function

$$Y(t) = \cos\frac{\omega_o t}{\pi}\ Si(\omega_s t-\omega_s g) - Si(\omega_s t-\omega_s g-\omega_s T_1) \tag{79}$$

For a rise time of .01 microsecond we would need an approximate bandwidth B = 160 megacycles. For very small rise times then we would be required to have a wide bandwidth giving rise to some loss in the signal to noise ratio.

The linear phase shift introduced by our system has added only a time delay and has not contributed to the distortion of our output. We note an unrealistic condition in that transients are available in the output prior to the application of the input. This is due to the fact that our system is not entirely realistic. It is impossible to have a system which gives us perfectly

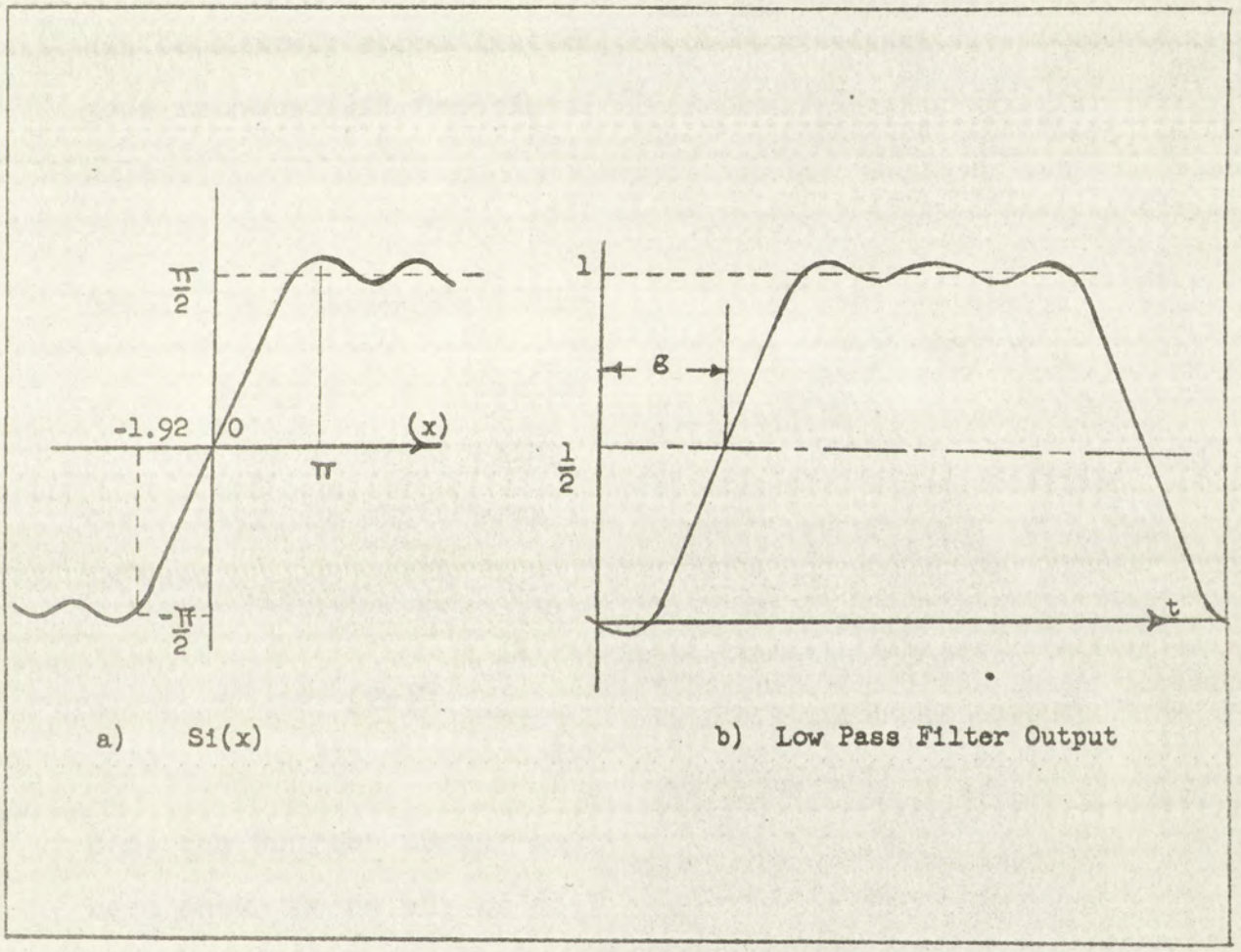

FIGURE 15

BANDWIDTH LIMITED RECTANGULAR PULSE

sharp cutoff frequency. In the case of a low pass filter it would necessitate an infinite number of sections to get an absolutely sharp cutoff at ω_s. This would then give an infinite time delay g. The relation between the amplitude and phase characteristics of our system cannot be physically realized. On the other hand these criteria can be closely approximated in practice and we have a good mathematical description of a "practical" rectangular pulse.

Range Accuracy of Rectangular Pulses

Using our expression for the range accuracy we will examine the accuracy using a rectangular pulse. For simplicity the continuous spectrum for a single pulse is used.

$$\beta^2 = (2\pi)^2 \frac{\int f^2 \left|U(f)\right|^2 df}{\int \left|U(f)\right|^2 df} \tag{80}$$

U(f) the Fourier transform of our pulse has previously been shown to be of the form

$$U(f) = \frac{k \sin \frac{\omega T_1}{2}}{\frac{\omega T_1}{2}} \tag{81}$$

where T_1 equals the pulse width. The integral in the denominator of the expression for β^2 will be finite

since our rectangular pulse will have finite energy. The integral in the numerator is evaluated as follows

$$(2\pi)^2 K^2 \int_{-\infty}^{\infty} \frac{f^2 \sin^2 \pi T_1 f}{\pi^2 T_1^2 f^2} \, df = K_1 \int_{-\infty}^{\infty} \sin^2 \pi T_1 f \, df \qquad (82)$$

the numerator therefore equals infinity. β will therefore equal infinity, but for an infinite bandwidth, our noise power $N = BN_0$ is also infinite, and our expression for δ_r is no longer valid.

In practice we are not capable of producing a perfect rectangular pulse and even if we were the receiver would not have the infinite bandwidth necessary to reproduce the echo faithfully. We continue then by analyzing the accuracy characteristics of our mathematical model of a practical rectangular pulse, where our expression for δ_r will hold.

Again the spectrum of the pulse is of the form

$$U(f) = \frac{K \sin \pi T_1 f}{\pi T_1 f} \qquad (83)$$

We will assume a specific bandwidth B and therefore

$$\beta^2 = \frac{(2\pi)^2 \int_{-\frac{B}{2}}^{\frac{B}{2}} \frac{f^2 \sin^2 \pi f T_1}{f^2 \pi^2 T_1^2} \, df}{\int_{-\frac{B}{2}}^{\frac{B}{2}} \frac{\sin^2 \pi f T_1}{f^2 \pi^2 T_1^2} \, df} \tag{84}$$

where T_1 is the pulsewidth of the perfect rectangular pulse prior to bandwidth limiting. For reasonable values of BT_1, T_1 is a good approximation to the width of the bandwidth limited pulse.

Letting $fT_1 = x$, $df = \frac{dx}{T_1}$

$$\beta^2 = \frac{4}{T_1^2} \frac{\int_{-\frac{B\pi T_1}{2}}^{\frac{B\pi T_1}{2}} \sin^2 x \, dx}{\int_{-\frac{B\pi T_1}{2}}^{\frac{B\pi T_1}{2}} \frac{\sin^2 x}{x^2} \, dx} \tag{85}$$

Evaluating the integral in the numerator we get

$$\frac{B\pi T_1}{2} - \frac{1}{2} \sin (B\pi T_1) \tag{86}$$

Evaluating the integral in the denominator we get

$$\int_{-\frac{B\pi T_1}{2}}^{\frac{B\pi T_1}{2}} \frac{(1-\cos 2x)}{2x^2}\, dx$$

$$= -\frac{2}{B\pi T_1} + \frac{2\cos B\pi T_1}{B\pi T_1} + 2\int_0^{B\pi T_1} \frac{\sin u}{u}\, du$$

Combining terms

$$\beta^2 = \frac{4}{T_1^2} \frac{\frac{B\pi T_1}{2} - \frac{1}{2}\sin B\pi T_1}{\frac{2}{B\pi T_1}[\cos(B\pi T_1) - 1] + 2\int_0^{B\pi T_1} \frac{\sin u}{u}\, du} \qquad (87)$$

$$\beta^2 = \frac{1}{T_1^2} \frac{B\pi T_1 - \sin B\pi T_1}{Si(B\pi T_1) + \frac{1}{B\pi T_1}(\cos B\pi T_1 - 1)} \qquad (88)$$

For large values of BT_1, β^2 approximately equals $\frac{2B}{T_1}$. Figure 16 is a graph of BT_1 versus $\beta^2 T_1^2$ and indicates that $\beta^2 = \frac{2B}{T_1}$ is a good approximation for large values of BT_1.

Making use of this approximation and substituting for β in our range accuracy expression we have the standard deviation of our time measurement as

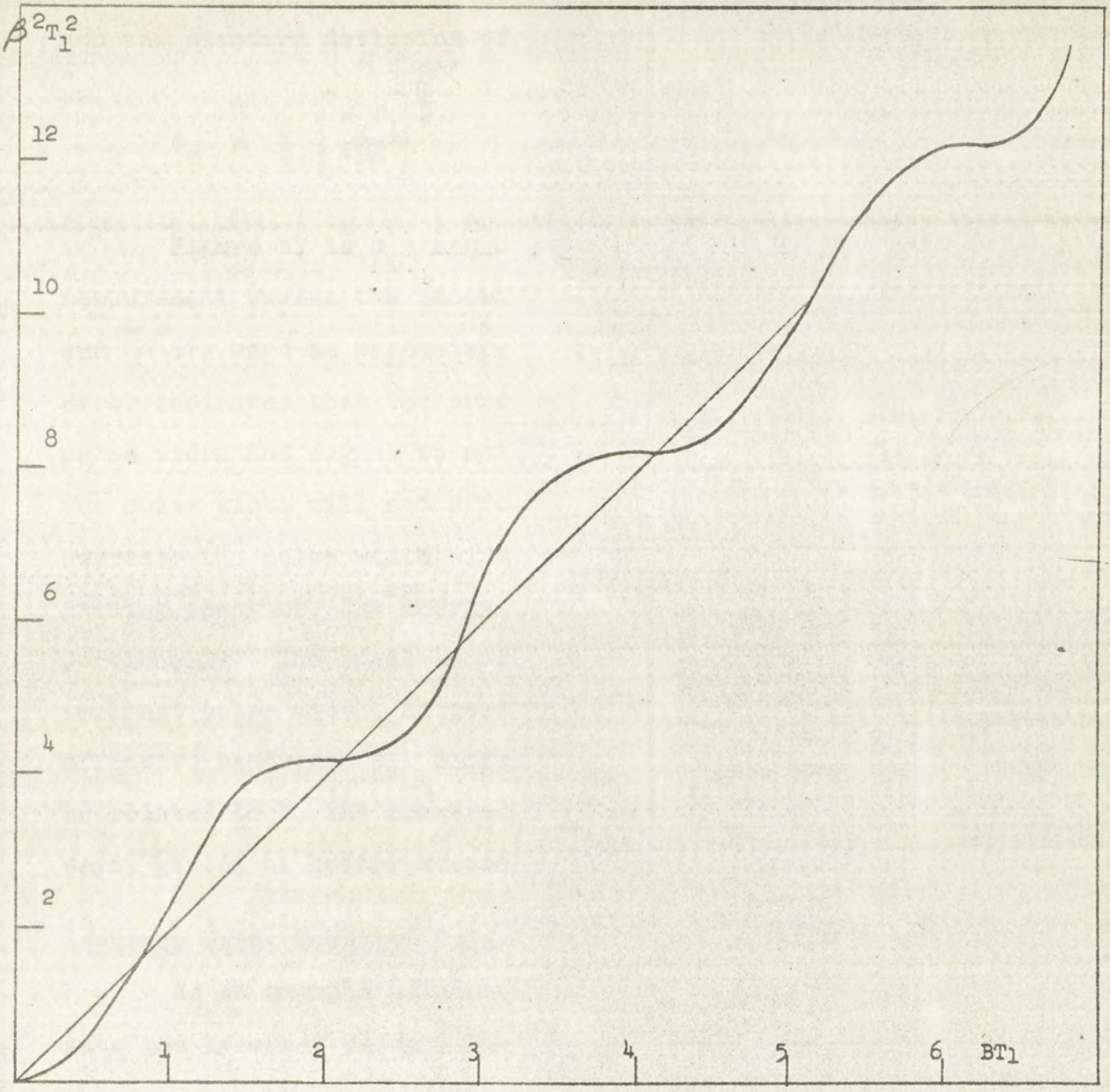

FIGURE 16

BT_1 VERSUS $\beta^2 T_1^2$ FOR A BANDWIDTH LIMITED PULSE

$$\delta_T = \left[\frac{N_o T_1}{4BE}\right]^{\frac{1}{2}} \tag{89}$$

and the standard deviation of our range measurement as

$$\delta_r = \frac{C}{2}\left[\frac{N_o T_1}{4BE}\right]^{\frac{1}{2}} \tag{90}$$

Figure 17 is a graph of the rms error in range measurement versus the bandwidth B. The pulse width T_1, and $\frac{E}{N_o}$ are used as parameters. Our expression for range error indicates that the error is dependent on the bandwidth, pulse width and signal to noise ratio. Simply decreasing the pulse width will not effect the accuracy for, as we decrease the pulse width with the signal amplitude remaining constant, the energy of the signal decreases proportionally. The ideal is of course the signal with the smallest pulse width, largest energy and the largest effective bandwidth β. Different types of pulses will be related to B, the spectral bandwidth in different ways, giving us better accuracy for the same bandwidth B.

Accuracy Using Gaussian Pulses

As an example of another type of pulse, we investigate the accuracy using a Gaussian pulse. The Gaussian

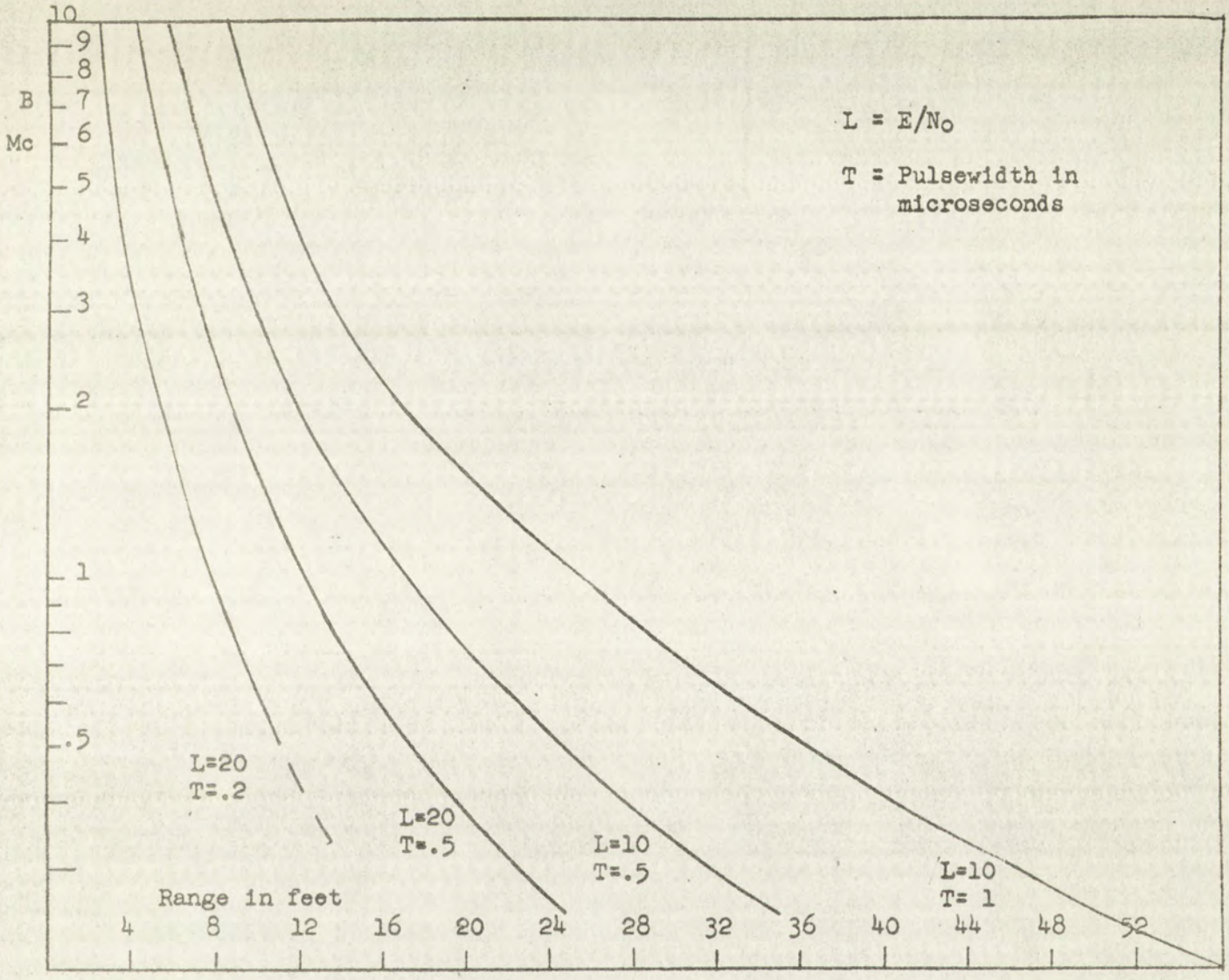

FIGURE 17

STANDARD DEVIATION IN RANGE ACCURACY VERSUS PULSE BANDWIDTH

pulse can be described

$$u(t) = K\ e^{-at^2} \tag{91}$$

where K is an arbitrary scale factor

$$U(f) = K\int_{-\infty}^{\infty} e^{-at^2}\ e^{-j\omega t}\ dt$$

$$U(f) = K\ (\frac{\pi}{a})^{\frac{1}{2}}\ \exp\ (-\frac{\omega^2}{4a}) \tag{92}$$

We then evaluate the effective bandwidth where

$$\beta^2 = \frac{(2\pi)^2 \int_{-\infty}^{\infty} f^2 \left|U(f)\right|^2\ df}{\int_{-\infty}^{\infty} \left|U(f)\right|^2\ df}$$

$$\beta^2 = \frac{(\frac{\pi a}{2})^{\frac{1}{2}}}{(\frac{\pi}{2a})^{\frac{1}{2}}} = a \tag{93}$$

We relate the constant a to the half power bandwidth B, as follows

$$U(f) = (\frac{\pi}{2})^{\frac{1}{2}}\ \exp\ (-\frac{\omega^2}{4a})$$

$$\frac{U^2(0)}{U^2(\frac{B}{2})} = \frac{1}{2} = \exp\ (-\frac{\pi^2 B^2}{2a}) \tag{94}$$

$$a = \frac{\pi^2 B^2}{1.386} \tag{95}$$

The standard deviation of our time measurement can then be expressed as

$$\delta_T = \frac{1.18}{B\left(\frac{2E}{N_o}\right)^{\frac{1}{2}}} \tag{96}$$

This expression for the rms time error for a Gaussian pulse differs from that of the rectangular pulse in several ways. The B here is not the frequency boundary for the wave but simply a parameter describing its spectrum. Since the spectral content falls off so rapidly as we move away from the carrier frequency, the exclusion of frequencies beyond some reasonably wide bandwidth would have little effect on our idealized expression. Since the half power pulse width is inversely proportional to the half power bandwidth, as we decrease the width of the pulse we accordingly increase our accuracy if we maintain the signal energy constant. A Gaussian pulse with a half power pulse width of .2 microseconds and $\frac{E}{N_o} = 50$ would have an rms range accuracy of

$$\delta_r = \frac{c}{2} \frac{T}{1.18\left(\frac{2E}{N_o}\right)^{\frac{1}{2}}} = 5.1 \text{ meter} \doteq 17 \text{ feet}$$

This is no improvement over the comparable rectangular pulse.

Accuracy Using Frequency Modulated Pulses

One of the problems of accurate tracking is the requirement for a small pulse width and a high peak power. There is often a system limitation on the usable peak power due to the breakdown of components in the radar at these peak ratings. To get around this limitation we can increase the energy per pulse if we increase the pulse length, but as previously mentioned the increase in pulse width and energy just balance in our expression for accuracy with no resultant accuracy gain. If we are able to increase the effective bandwidth β while maintaining constant the actual bandwidth B and pulse width T_1 we will increase the accuracy of our range determination. To increase β some kind of modulation of the signal must be used. Frequency or phase modulation is often used for this purpose resulting in "Pulse Compression".

To demonstrate the effect of pulse compression on our accuracy we evaluate a rectangular pulse of width T_1 and modulating the carrier frequency linearly over a bandwidth B we get

$$u(t) = A \cos (2\pi f_o t + Bt^2) \qquad (97)$$

C. E. Cook[24] analyzes the spectra and time functions of pulse compression waveforms. For BT_1 large the spectrum of a linear FM pulse compression waveform approaches a rectangular

---

24. C. E. Cook, "Pulse Compression-Key to More Efficient Radar Transmission", Proc. IRE Vol 48, pp310-316 March 1960

distribution. The effective spectrum then approaches,

$$\lim_{BT\to\infty} \beta^2 = \frac{(2\pi)^2 \int_{-\frac{B}{2}}^{\frac{B}{2}} f^2\, df}{\int_{-\frac{B}{2}}^{\frac{B}{2}} df} = \frac{\pi^2 B^2}{3} \qquad (98)$$

therefore

$$\delta_T = \frac{(3)^{\frac{1}{2}}}{B\left(\frac{2E}{N_o}\right)^{\frac{1}{2}}} \qquad (99)$$

Comparing this to the accuracy determined for a "practical" rectangular pulse we get (100)

$$\frac{\text{Rectangular pulse rms error}}{\text{FM pulse compression error}} = \left[\frac{N_o T_1}{4BE} \cdot \frac{6E}{N_o}\right]^{\frac{1}{2}} \pi B$$

$$= (BT_1)^{\frac{1}{2}} \frac{\pi}{\sqrt{6}}$$

For BT_1 equal to 50 the pulse compression wave form is approximately nine times more accurate than the practical rectangular waveform. From Figure 14 and the errors in range associated with our practical rectangular pulse we can see that this type of pulse compression reduces our theoretical accuracy limitations to a maximum in the order

of a few feet. Pulse compression also offers us the opportunity of using a longer pulse of higher energy without losing any accuracy. As we increase our energy we increase the range over which we can be accurate.

Many different types of pulses and modulations can be analyzed. The few examples demonstrated here indicate that theoretical range errors for pulse radar can be reduced by proper pulse techniques to values below those small range errors introduced by the change in velocity of our wave in the atmosphere.

This analysis has made use of our information theory approach to pinpoint the factors that influence radar range accuracy. The relationships between pulse width, bandwidth and signal to noise ratio and their effect on accuracy was demonstrated for various types of pulses.

From our knowledge of the parameters involved the atmospheric refraction of a wave should have no appreciable effect on the inherent accuracy of our radar in any region where ray theory is applicable and the refraction is not frequency sensitive. Each frequency component will travel the same path, experience the same bending and travel at the same velocity. Their resultant wave shape is unchanged.

CHAPTER V

THE EFFECT OF ABSORPTION AND DISPERSION ON RADAR PROPAGATION

The Atmosphere as an Electromagnetic Medium

The index of refraction of the atmosphere is dependent upon the molecular constitution of the atmosphere. The microscopic formulas for the index were briefly discussed in Chapter II. To evaluate the effects of the variation of the index of refraction with frequency we must consider the mathematical description of the atmosphere as a medium for electromagnetic propagation. An electromagnetic field can be described by the four vectors $\underline{E}$, $\underline{B}$, $\underline{D}$, and $\underline{H}$ where $\underline{E}$ and $\underline{H}$ are the electric and magnetic field intensities, $\underline{D}$ the electric displacement and $\underline{B}$ the magnetic induction. These vectors are related by Maxwell's equations and the conditions imposed by the medium of propagation. The electric displacement is a function of $\underline{E}$ and the magnetic intensity $\underline{H}$ is a function of $\underline{B}$*. The general assumption is that of an

---

* The assumption of $\underline{D}$ as a function of $\underline{E}$, and $\underline{H}$ as a function of $\underline{B}$ does not infer that either $\underline{E}$ or $\underline{B}$ are causal factors but only that a relationship between the vectors exists. The development follows that of J. K. Stratton, "Electromagnetic Waves", McGraw Hill Book Company, pp10-12.

isotropic medium where the relationships between these vectors are linear. In this case the factors ϵ and μ the inductive capacities or permittivity and permability are defined by

$$\underline{D} = \epsilon \underline{E} \qquad\qquad \mu \underline{H} = \underline{B} \tag{101}$$

In free space $\mu = \mu_o$, $\epsilon = \epsilon_o$ and the dimensionless specific inductive capacities k_ϵ, k_m are defined as

$$k_\epsilon = \frac{\epsilon}{\epsilon_o} \qquad\qquad k_m = \frac{\mu}{\mu_o} \tag{102}$$

In general the inductive capacities are scalar functions of position which characterize the electromagnetic properties of our medium. The medium is further described by the relation between the current density $\underline{J}$ and the electric field intensity.

While the distribution of current in our ionized gas may depend on $\underline{H}$, $\underline{J}$ is a linear function of $\underline{E}$ for a wide range of conditions.

$$\underline{J} = \sigma \underline{E} \tag{103}$$

where σ is defined as the conductivity of the medium. When k_ϵ and k_m are independent of the frequency of the applied field and the medium is nonconducting, the different frequency components of a pulsed signal are propagated with the same velocity. The presence of non zero conductivity makes the Phase velocity a function of frequency and as the harmonic

components are propagated through some distance a relative phase shift occurs so that the addition of these harmonics at a distant point leads to a modified and perhaps unrecognizable reproduction of the original signal. This breakdown in waveshape is called dispersion.

The frequency depedence of k_ϵ or k_m will have a similar effect on the phase velocity causing it to become frequency sensitive. At frequencies below 1 KMc, k_ϵ and k_m are essentially independent of frequency and there is no dispersion of an electromagnetic wave.

To consider the effects of atmospheric conduction we use the usual development for a plane wave harmonic in time.

$$\underline{E} = \Psi_1(x)\ \Psi_2(t) \tag{104}$$

From Maxwell's Equations

$$\frac{\partial^2 \underline{E}}{\partial Z^2} = \mu\epsilon \frac{\partial^2 \underline{E}}{\partial t^2} + \mu\sigma \frac{\partial \underline{E}}{\partial t} \tag{105}$$

$$-K^2 = \frac{1}{\Psi_1} \frac{d^2\Psi_1}{dz^2} = \frac{\mu\epsilon}{\Psi_2} \frac{d^2\Psi_2}{dt^2} + \frac{\mu\sigma}{\Psi_2} \frac{d\Psi_2}{dt}$$

Taking the exponential solution for Ψ_2

$$\Psi_2 = Ce^{-pt}$$

$$\Psi_1 = Ae^{jKZ} + Be^{-jKZ} \tag{106}$$

solving

$$p^2 - (\frac{\sigma}{\epsilon})p + \frac{K^2}{\mu\epsilon} = 0$$

For our plane wave harmonic in time $p = j\omega$ and solving for K

$$K^2 = \omega^2\mu\epsilon + j\mu\omega\sigma$$

$$K = \alpha + j\beta \tag{108}$$

$$\alpha^2 - \beta^2 + j2\alpha\beta = \omega^2\mu\epsilon + j\omega\mu\sigma$$

solving for α

$$\alpha = \omega\left[(\frac{\mu\epsilon}{2})\left[(1 + \frac{\sigma^2}{\epsilon^2\omega^2})^{\frac{1}{2}} + 1\right]\right]^{\frac{1}{2}} \tag{109}$$

since v_p the phase velocity equals $\frac{\omega}{a}$

$$v_p = \left[\frac{\mu\epsilon}{2}\left[(1 + \frac{\sigma^2}{\epsilon^2\omega^2})^{\frac{1}{2}} + 1\right]\right]^{-\frac{1}{2}} \tag{110}$$

At normal radar frequencies and with the low conductivity of the atmosphere $\frac{\sigma^2}{\epsilon^2\omega^2}$ is very much less than one. Expanding v_p by the use of a power series

$$v_p = \left[(\mu\epsilon)^{\frac{1}{2}}(1 + \frac{1}{8}\frac{\sigma^2}{\epsilon^2\omega^2} + \ldots.)\right]^{-1} \tag{111}$$

Even after this expansion the second term is generally negligible and the conductivity of the atmosphere can be neglected as a contributing factor to dispersion of a radar signal.

Molecular Absorption and Dispersion

The dispersive characteristic of the atmosphere can then be attributed to the dependence of the inductive capacity on frequency. This frequency dependence is a result of the excitation of the molecular oscillators by the incident field. The first noticeable evidence of a change of the specific inductive capacity of the atmosphere occurs in the vicinity of 15 KMc due to absorption by water vapor[25]. At frequencies lower than 15 KMc the attenuation by atmospheric gases will be less than .02 db/KM[24]. Investigation of the usual atmosphere reveals that only water vapor has a permanent electric dipole moment and energy spacings within the molecular energy spectrum of the appropriate levels to cause significant change in the index below wave lengths of 1 mm (approximately 300 KMc). Oxygen on the other hand has a permanent magnetic moment which is capable of absorbing microwaves, and the resonant effect at about 60 KMc makes the absorption by oxygen extremely important. These two gases are the only absorbers that need to be considered in the frequency range of interest.

The atmospheric molecules of oxygen and water vapor behave like dipoles. They react to the passing field by rotating or oscillating in many different ways. To each of the possible modes of vibration there belongs an energy level of the molecule. There is an extremely large number of

---

25. L. Battan, "Radar Meterorology", University of Chicago Press, pp 42-44, 1959
26. Ibid
27. J.H. VanVleck, "Absorption of Microwaves by Oxygen", Physics Review, LXXI, 1947.

energy levels that are very closely spaced. If the energy difference between two levels is $\Delta\mathcal{E}$, a passing wave of the correct frequency $f = \frac{\Delta\mathcal{E}}{h}$ (h is Planck's constant) will shift the molecule to the higher energy level.

Our incoming wave therefore contributes discrete amounts of energy to the atmospheric molecules keeping them in a constant state of transition. The molecule will reradiate the energy in a random manner when it drops back to the lower level. This reradiation will not reinforce the exciting wave and the total effect is therefore one of absorption. Molecular damping forces occur which control the width and height of this resonance curve. Using the model of a molecule as a damped oscillator subjected to a driving force, the classical dispersion formula can be developed in terms of the electric field $\underline{E}$ and the polarization, $\underline{P}$[28].

$$\underline{P} = \frac{\frac{Ne^2}{m} \cdot \underline{E}}{\omega_o^2 - \omega^2 - j4\pi r} \qquad (112)$$

where N is the number of oscillators per unit volume, e the electron charge, m the mass of the electron ω_o the resonant frequency and r is a term due to the friction or damping force. For a number of oscillators of different type

---

28. A. Von Hippel, "Dielectics and Waves", John Wiley and Sons, Inc. New York, pp 100-104, 1954

$$\underline{P} = \sum_s \frac{\epsilon_o a_s^2 \underline{E}}{\omega_s^2 - \omega^2 - j\omega 4\pi r_s} \tag{113}$$

where a_s^2 equals $\frac{N_s e^2}{\epsilon_o m_s}$. Since $\underline{P}$ is defined equal to $(k-1)\epsilon_o \underline{E}$ we have a complex value of the relative inductive capacity k.

$$k = 1 + \sum_s \frac{a_s^2}{\omega_s^2 - \omega^2 - j4\pi\omega r_s} \tag{114}$$

Far below its resonant frequency (ω very much less than ω_s) each oscillator, type s, will make a constant contribution

$$\frac{a_s^2}{\omega_s^2}$$

to the static inductive capacity of the medium. Considering the lowest atmospheric resonances we lump the effect of vacuum and the remaining resonator types into a constant contribution

$$A = 1 + \sum_s \frac{a_s^2}{\omega_s^2} \tag{115}$$

then

$$k = A + \frac{a_o^2}{\omega_o^2 - \omega^2 - j4\pi\omega r_o} \tag{116}$$

In the vicinity of resonance ω approximately equals ω_o.

Then letting $(\omega_o - \omega) = \Delta\omega$, and $B = \frac{a_o^2}{4\pi f_o}$

$$k = A + \frac{B}{\Delta f + jr_o} \qquad \Delta\omega = 2\pi\Delta f$$

$$k = A + \frac{B\Delta f}{\Delta f^2 + r_o^2} - \frac{j\,Br_o}{\Delta f^2 + r_o^2} \tag{117}$$

The real part of the complex relative inductive capacity describes the dispersive characteristics of the medium, and the imaginary part describes the absorption near resonance.

$$k = k' + jk''$$

$$k' = A + \frac{B\Delta f}{\Delta f^2 + r_o^2} \tag{118}$$

$$k'' = \frac{Br_o}{\Delta f^2 + r_o^2}$$

For very small values of (n^2-1), n equals approximately the square root of k'. The values of (n^2-1) for frequencies of interest will always be less than 10^{-3} and this is a good approximation.

To relate k" to a usual method of measuring absorption we return to the descriptive wave equation

$$\frac{\partial^2 \underline{E}}{\partial Z^2} = \epsilon_o \mu_o K \frac{\partial^2 \underline{E}}{\partial t^2} \tag{119}$$

where the term involving the conductivity has been set to zero. The solution is

$$\underline{E} = \underline{E}_o \exp (jKZ - j\omega t) \qquad (120)$$

where

$$K = \frac{\omega}{c} \sqrt{k} = \frac{\omega}{c} (k' + k'')^{\frac{1}{2}}$$

c = the speed of light. Since k' equals approximately one and is much greater than k" we expand (k' + k") retaining the first two terms of a binomial expansion and

$$K \doteq \frac{\omega}{c} (k' + \frac{jk''}{2}) \qquad (121)$$

Defining γ as the absorption loss in db per kilometer we have

$$\gamma = 10 \log \frac{P(z=0)}{P(z=km)}$$

$$\gamma = 10 \log e^{-2j \frac{(jk''\omega)}{2c}} \quad 10^5$$

$$\gamma = 10^6 (\frac{2\pi}{\lambda}) k'' \log_{10} e \qquad (122)$$

where λ is the wave length, in centimeters. We have used the classical dispersion formula. In the quantum mechanical development the resonant absorption corresponds to a quantum transition from a lower to an allowed higher energy state. We are concerned with the number of atoms available for this transition, (i.e. the difference between the population of each state) rather than just the number of dispersion electrons

available. While the nomenclature is of course different the quantum mechanical approach leads to the same formulas for k' and k" in the vicinity of resonance.[29]

Dispersion and Absorption By Oxygen and Water Vapor in the Atmosphere

We now apply our knowledge of the atmosphere as an electromagnetic medium to evaluate the specific effects of atmospheric dispersion and absorption in the microwave range. Where

$$k' = A + B \frac{(\Delta f)}{\Delta f^2 + r^2}$$

$$k'' = \frac{Br}{\Delta f^2 + r^2}$$

The maximum value of absorption occurs when f = 0 and then

$$k'' \text{ max} = \frac{B}{r} \qquad (123)$$

The maximum and minimum values of k' occur at f_o or -r where

$$k' = A \pm \frac{Br}{2r^2} = A \pm \frac{B}{2r} \qquad (124)$$

The difference between the maximum and minimum values of k' then is just equal to the value of k" max., $\frac{B}{r}$.

Making use of the known information concerning oxygen

---

29. D. E. Kerr, op cit. Chapter 8.1, pp 641-646.

$f_o = 60KMc \qquad r = 6000/sec$

and for water

$f_o = 22.4KMc \quad r = 3000/sec$

Having fairly accurate measurements of the absorption for both water and oxygen in the frequency range of interest we can evaluate the expressions for k' and k". At f equal to the resonant frequency for oxygen, 60KMc, the absorption per kilometer is about 15db per kilometer. Assuming in this case a standard pressure of 760 mm and a temperature of 20° Centigrade.

$$= \frac{27.3 \times 10^5}{\lambda} \quad k'' = 15db \text{ per Km}$$

$$\max k''_{ox} = .275 \times 10^5$$

$$B_{ox} = \max k''_{ox} r_{ox} = 1650 \qquad (125)$$

For water at the resonant frequency of 22.4 KMc, $\gamma_H = .020$ db per Km/per gram per cubic meter. Using a saturated maximum value of 17 grams of H_2O per cubic meter

$$\gamma = .34 = 27.3 \times 10^5 \frac{k''_H}{\lambda_o}$$

$$\max k'' = .168 \times 10^{-6} = \frac{B_H}{r_H}$$

$$B_H = 505 \qquad (126)$$

The difference between peak values of k' is equal to k" max. For oxygen $\Delta k' \doteq .27 \times 10^{-5}$ and for uncondensed water vapor $\Delta k' \doteq .17 \times 10^{-6}$. These spreads are based on sea level conditions. The absorption by oxygen is proportional to the quotient of density by temperature, and will decrease at high altitudes[29]. The absorption by water vapor is directly proportional to water vapor content, and will also decrease at high altitudes[25]. The spreads in index value between different frequencies will then derecase on the average with height and an average value of B will be accurate enough for our purposes.

Looking at the maximum variations with frequency of k' we see that they are extremely small. As pointed out by Van Vleck[27] the figures indicate that while the effects of these two molecular resonances are important from the standpoint of absorption they are practically negligible as far as dispersion is concerned.

A maximum variation from the static value of the index would be in the vicinity of one or two times 10^{-6} for frequencies around 60KMc.

To analyze the effect of dispersion on a rectangular pulse we choose a 15 KMc carrier frequency and an unreasonably large bandwidth of 200Mc, plus or minus 100Mc around the carrier. A measure of our distortion due to the frequency

sensitive medium is the phase shift between the carrier frequency component and the outermost harmonic.

Over a distance d the difference between a harmonic component and the reference with respect to time of arrival will be $\Delta\tau = d_1 \left(\frac{1}{v_1} - \frac{1}{v_2}\right) \doteq \frac{d_1}{v}\left(\frac{\Delta v}{v}\right)$ (127)

where Δv is the difference in velocity due to the different frequencies involved. Letting v_c = the carrier velocity and v_s = the velocity of the uppermost frequency component of our signal

$$\Delta v = v_c - v_s$$

$$\frac{\Delta v}{v_s} = \frac{v_c}{v_s} - 1 = \frac{n_s}{n_c} - 1 \qquad (128)$$

with $n = (k')^{\frac{1}{2}}$

(128)

$$n_s = \left[\frac{+ B_1(f_1 - f_s)}{f_1^2 + (f_s - f_1)^2} + \frac{B_2(f_2 - f_s)}{f_2^2 + (f_2 - f_s)^2} + A\right]^{\frac{1}{2}}$$

$$n_c = \left[\frac{+ B_1(f_1 - f_s)}{f_1^2 + (f_r - f_1)^2} + \frac{B_2(f_2 - f_s)}{f_2^2 + (f_{2^-} f_r)^2} + A\right]^{\frac{1}{2}}$$

where the subscript 1 indicates parameters of oxygen, 2 indicates parameters of water, r indicates the reference frequency, and s indicates the upper sideband frequency 15.1 KMc. All the contributions of vacuum and the higher resonant

types we lump into A, with a maximum value of A around 1.001. Using this maximum value of A and substituting we get

$$n_s = 1.00050004815$$

$$n_c = 1.00050004780$$

and

$$\frac{\Delta v}{v} = .35 \times 10^{-9}$$

The difference in arrival time between the boundary frequency components will be

$$t_2 - t_1 = d_1 \left(\frac{1}{v_1} - \frac{1}{v_2} \right) \qquad (130)$$

$$t_2 - t_1 \doteq \frac{d_1}{v} \left(\frac{\Delta v}{v} \right)$$

for a path length of 300 Km

$$t_2 - t_1 = .3 \times 10^{-6} \text{ microseconds}$$

This will lead to no noticeable effect on our wave shape. This figure is based on the use of the sea level spread in index over the entire path. Use of an average spread would decrease this value even further. At 60KMc where we will experience maximum dispersion in the frequency range of interest $t_2 - t_1$ is less than 10^{-3} microseconds. A formal analysis of the effect on the wave shape would involve reformation of the wave including the change in phase characteristic over a certain frequency band for the given path. For these small changes the accuracy of determination

of the pulse edge will not be decreased by any more than $\Delta\tau$. In terms of range accuracy then, a maximum error at 60 KMc would be less than a foot.

We cannot assume there will be no change in our wave shape without also considering the effect of the absorption. The frequency extremes of our signal will encounter different absorptions due to the frequency sensitive nature of the absorption. From figure 10 of Chapter II the two way absorption at zero elevation angle is approximately 18 db, for 15KMc. For 15.1 KMc the upper boundary of our theoretical signal the absorption is 18.3 db per Kilometer. Within this range the attenuation is roughly linear, the ratio of the attenuations of the upper and lower sidebands being 1.032 and .968 with respect to the carrier attenuation.

To examine the effects of this frequency sensitive absorption on our wave shape we consider the atmosphere as a system having a linear frequency characteristic between our two sidebands as illustrated in figure 18.

For ω_c equal 2π (15KMc) and ω_s equal to 2π(.1 KMc)

$$F(\omega) = A\omega + K$$

where $A = \frac{.032}{\omega_s}$ $\qquad$ $K = 1 + \frac{.032\omega_c}{\omega_s}$

We will assume we start with a perfect rectangular pulse envelope and our high frequency carrier. The fourier transform for this signal is

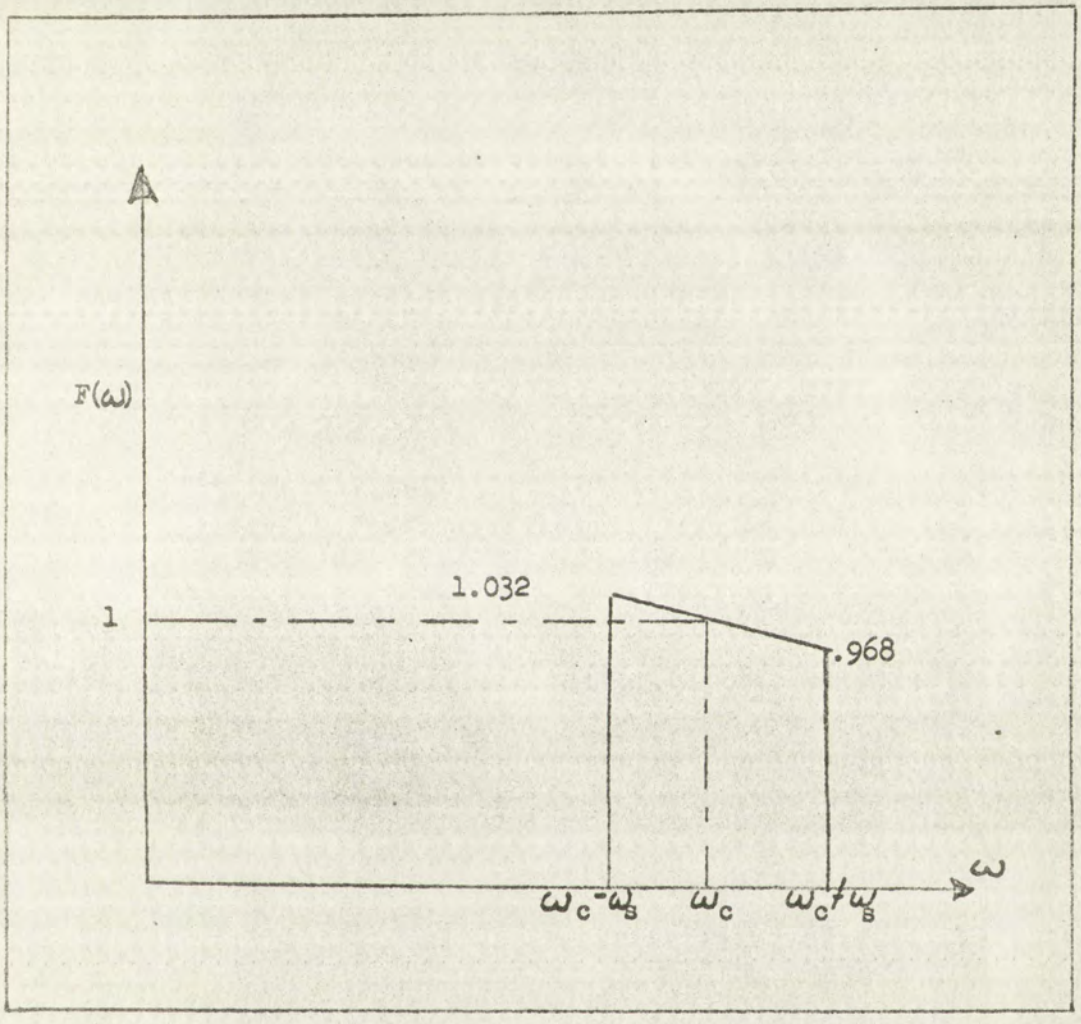

FIGURE 18

SIMULATED ATMOSPHERIC FREQUENCY CHARACTERISTIC

$$a(\omega) = \frac{1}{\pi} \left[\frac{\sin (\omega-\omega_c)\frac{T}{2}}{\omega - \omega_c} + \frac{\sin (\omega+\omega_c) \frac{T}{2}}{\omega + \omega_c} \right] \qquad (131)$$

where T = the pulse width. Our output response from our simulated atmospheric system is then

$$G(t) = \int_0^\infty a(\omega)\, F(\omega) \cos \omega t \, d\omega$$

$$= \frac{1}{\pi} \int_{\omega_c-\omega_s}^{\omega_c+\omega_s} \frac{\sin(\omega-\omega_c) \frac{T}{2}}{\omega-\omega_c} (A\omega+k) \cos\omega t \, d\omega \qquad (132)$$

where the terms with $\omega+\omega_c$ in the denominator have been discarded as negligible compared to the $\omega - \omega_c$ terms.

$$G(t) = \frac{K}{\pi} \int_{\omega_c-\omega_s}^{\omega_c+\omega_s} \frac{\sin(\omega-\omega_c) \frac{T}{2}}{\omega - \omega_c} \cos\omega t \, d\omega$$

$$+ \frac{A}{\pi} \int_{\omega_c-\omega_s}^{\omega_c+\omega_s} \frac{\omega \sin (\omega-\omega_c) \frac{T}{2}}{\omega - \omega_c} \cos\omega t \, d\omega \qquad (132)$$

Examining the first of these two terms it can be shown that it equals

$$\frac{K}{\pi} \cos\omega_c t \left[Si(\omega_s(t + \tfrac{T}{2})) - Si(\omega_s(t - \tfrac{T}{2})) \right] \qquad (133)$$

and substituting for the value of K

$$\frac{1}{\pi} \cos \omega_c t \left[Si\left(\omega_s \left(\frac{T}{2} + t \right) \right) - Si\left(\omega_s \left(t - \frac{T}{2}\right) \right) \right] \qquad (134)$$

$$+ \frac{.032\omega_c}{\pi\omega_s} \cos\omega_c t \left[Si\left(\omega_s \left(t + \frac{T}{2}\right) \right) - Si\left(\omega_s \left(t + \frac{T}{2}\right) \right) \right]$$

Examining the second of the two terms making up G(t) it can be shown equal to

$$A \frac{\omega_c}{\pi} \cos\omega_c t \left[Si\left(\omega_s \left(t + \frac{T}{2}\right) \right) - Si\left(\omega_s \left(t - \frac{T}{2}\right) \right) \right] \qquad (135)$$

$$+ \frac{A}{\pi} \sin\omega_c t \left[\frac{Sin\left(\omega_s \left(t + \frac{T}{2}\right) \right)}{t + \frac{T}{2}} - \frac{Sin\left(\omega_s \left(t - \frac{T}{2}\right) \right)}{t - \frac{T}{2}} \right]$$

Combining terms to get G(t)

$$G(t) = \frac{1}{\pi} \cos\omega_c t \left[Si\left(\omega_s \left(t + \frac{T}{2}\right) \right) - Si\left(\omega_s \left(t - \frac{T}{2}\right) \right) \right] \qquad (136)$$

$$- \frac{.032}{\pi} \sin\omega_c t \left[\frac{\sin\omega_s \left(t + \frac{T}{2}\right)}{\omega_s \left(t + \frac{T}{2}\right)} - \frac{\sin\omega_s \left(t - \frac{T}{2}\right)}{\omega_s \left(t - \frac{T}{2}\right)} \right]$$

The first term is our practical rectangular pulse and the second the term due to the distortion introduced by our frequency sensitive atmosphere. If the pulse is wide enough

to ignore the effect of the lagging edge distortion term we will have the new leading edge represented by

$$\frac{1}{\pi}\left[\mathrm{Si}\left[\omega_s\left(t+\frac{T}{2}\right)+\frac{\pi}{2}\right]\cos\omega_c t\right] - .\frac{032}{\pi}\,\frac{\sin\omega_s\left(t+\frac{T}{2}\right)}{\omega_s\left(t+\frac{T}{2}\right)}\sin\omega_c t \qquad (137)$$

This will decrease the value of our pulse by a maximum of $\frac{.032}{\pi}$ at $t = \frac{T}{2}$.

$$\frac{\sin\omega_s\left(t+\frac{T}{2}\right)}{\omega_s\left(t+\frac{T}{2}\right)} = \text{zero at } \omega_s\left(t+\frac{T}{2}\right) = \pi \qquad (138)$$

or

$$t = \frac{\pi}{\omega_s} - \frac{T}{2}$$

The distortion is therefore zero at this value of t. The peak of our practical pulse also occurs at t equal to $\frac{\pi}{\omega_s} - \frac{T}{2}$. Figure 19 shows an exaggerated comparison of our practical pulse and G(t) our practical pulse after frequency distortion. As can be seen the introduction of this distortion, will to some extent change our wave shape. For a system where range is determined by measuring the time the return signal crosses some threshold level, a time measurement error ΔT will occur having a maximum value in the vicinity of the center of our leading edge. This maximum is approximately 1% of the rise time for our 15KMc signal. For most practical pulses then

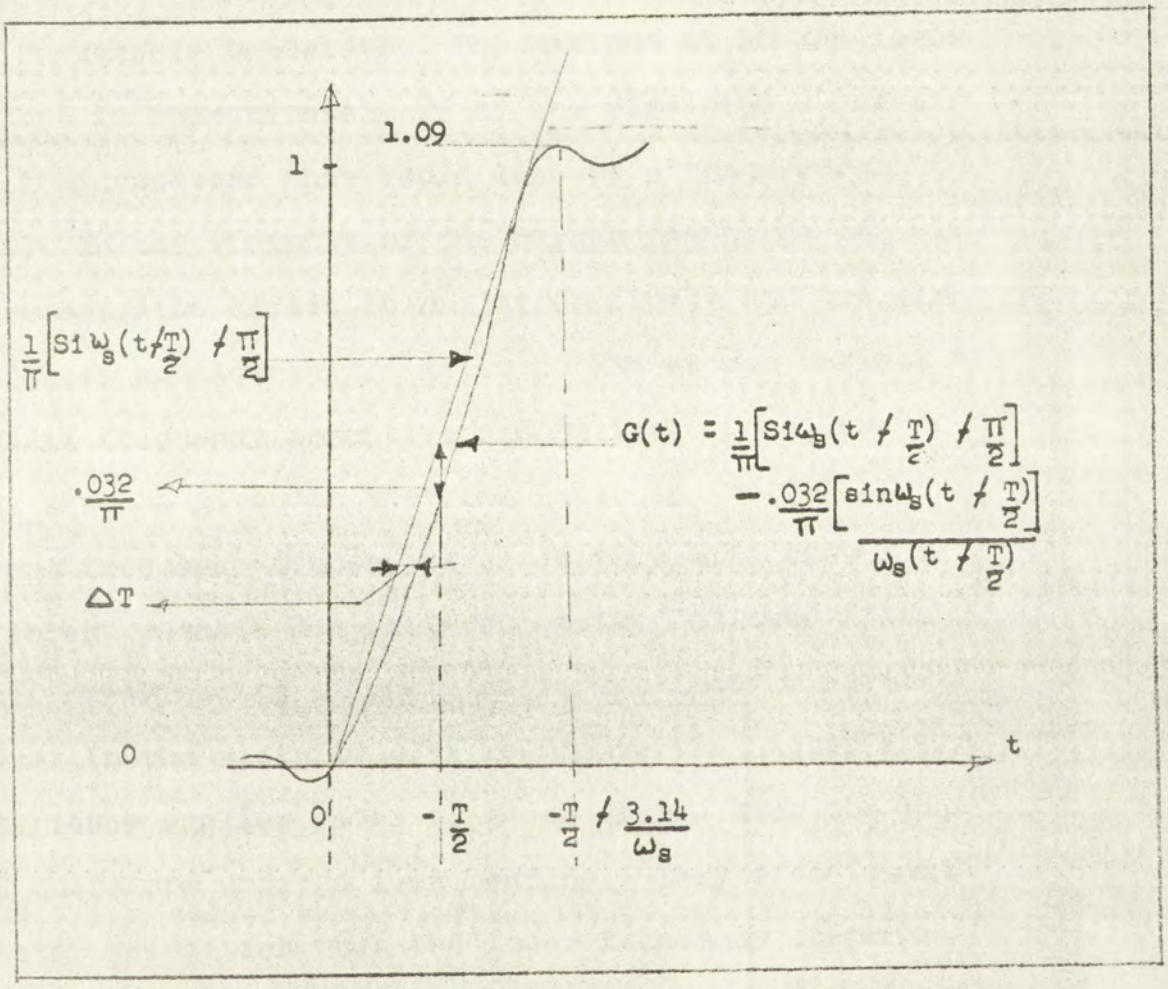

FIGURE 19

ILLUSTRATION OF G(t) VERSUS TIME

this will lead to negligible range errors. The magnitude of the distortion term is dependent on the slope of $F(\omega)$. In the vicinity of the H_2O resonance this reaches a maximum at about 20 KMc and the slope is still roughly linear, over any reasonable bandwidth. The maximum at 20 KMc leads to a ΔT that is approximately 8% of the rise time. For a rise time of .1 microsecond this would lead to a range error of several feet. In the vicinity of the oxygen resonance the slope increases, the effect is no longer linear, and the distortion increases considerably. Below 50 KMc we can neglect the effect of this frequency sensitive absorption. Consideration must also be given to the time lapse in arrival of the different frequency components since they will travel slightly different paths. The different paths followed arise due to their experiencing slightly different index distributions.

In the vicinity of a resonance the higher frequencies experience smaller rates of index change over the path length and therefore undergo less bending. They also travel at greater velocities than the lower frequency components. This effect causes a dispersion in space as well as time. The phenomena is the same in regions of normal dispersion with the roles of the higher and lower frequency components interchanged.

In the frequency region where dispersion occurs the higher frequency radiation from an isotropic source would reach a given point in space in less time than the lower frequency components. This is due to the fact that the high frequency radiation will travel straighter and faster.

Since the difference in velocities have been shown to be small, the difference in arrival times would be the difference in path length divided by an average velocity.

For a point target at the outer edge of the atmosphere the maximum difference in launch angle calculated for frequencies in the vicinity of the oxygen resonance was less than .02 milliradians. The reference launch angle was .025 radians, the frequency boundaries plus and minus 100 Mc around 60 KMc. The gradient was assumed constant with height. It should be noted that the maximum variations in index due to the frequency spread would be beyond our present high altitude index measurement capability. They therefore have less effect than the present indeterminancy of the index profile. The path length was computed for a signal with .01 radians between the tangent to the launch ray and straight line path to the target. The path length for a signal with .01 + .00002 radians between the tangent to the launch ray and the straight line path was computed. The actual paths were assumed as arcs of a circle. The true slant range to the target was taken = 1000 K ft.

From Figure 20 where d = 1000 K ft, the launch angle $\alpha = .01$

$\Delta\alpha = .02 \times 10^{-3}$, $\Psi = .025$, R = the radius of curvature.

$$S_1 - d = R\left(\theta - 2\sin\frac{\theta}{2}\right) \tag{138}$$

$$= R\left[\theta - 2\left(\frac{\theta}{2}\right) - \frac{1}{3!}\left(\frac{\theta}{2}\right)^3 + \ldots\right]$$

with $\frac{\theta}{2} = \alpha = .01$ radians

$$R \doteq \frac{d}{\theta} = 5 \times 10^7 \tag{139}$$

$$S_1 - d = 5 \times 10^7 \cdot 1/3\ (10^{-6}) \tag{140}$$

$$= 16.666\ldots$$

with $\frac{\theta}{2} = \alpha = .01002$

$$S_2 - d = 5 \times 10^7\left[1/3\ (.01002)^3\right]$$

$$S_2 - S_1 = .102 \text{ feet} \tag{141}$$

or a maximum difference in arrival time of frequency components of about .0001 microsecond.

The use of 60 KMc gave us the region of maximum dispersion for pulsed radar in the frequency area of interest. The wide bandwidth chosen also contributed to maximizing the dispersive effect. The assumption that the paths were arcs of circles as well as the uncertainty in the variation of the index in the resonant area make the calculation approximate.

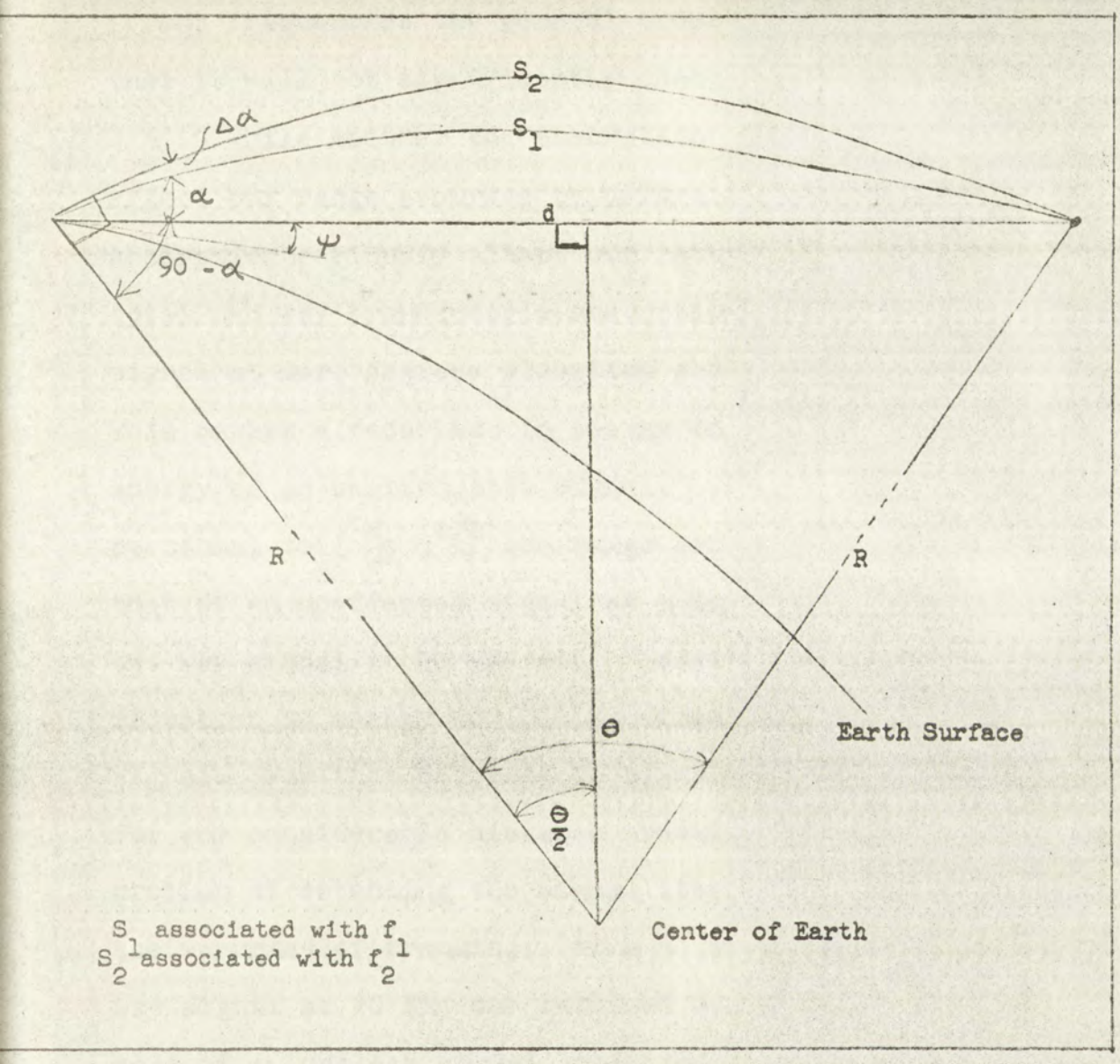

FIGURE 20

ILLUSTRATION OF DIFFERENT RAY PATHS(EXAGGERATED)
DUE TO DIFFERENT INDEX PROFILES

Having taken a maximum launch angle difference for the different frequencies the general order of the effect indicates that it will not significantly change our waveshape.

While neither the absorption nor dispersion seriously effect our range accuracy by deforming our waveshape the absorption seriously alters our returned signal energy. A total two way tropospheric absorption of 18 db occurs for a signal at zero degrees elevation and 15 KMc (see Figure 21). This causes a reduction in energy to 0.0167 times the return energy of an unattenuated signal. The error being proportional to $\left(\frac{N_o}{E}\right)^{1/2}$ the range error would be about 8 times that of an uneffected signal at a lower frequency. For a two way signal at 20 KMc and 0^o elevation angle there is a reduction in energy to .000625 times that of an unattenuated signal. For this decrease in signal to noise energy we would, for any considerable distance tracking, be faced with the problem of detecting the signal itself rather than determining the accuracy of tracking. At a 3^o elevation angle for a two way signal at 20 KMc the returned energy would be .055 times that of a lossless signal, pointing out the importance of the elevation angle. Figure 21 is a graph of the relative energy loss versus frequency.

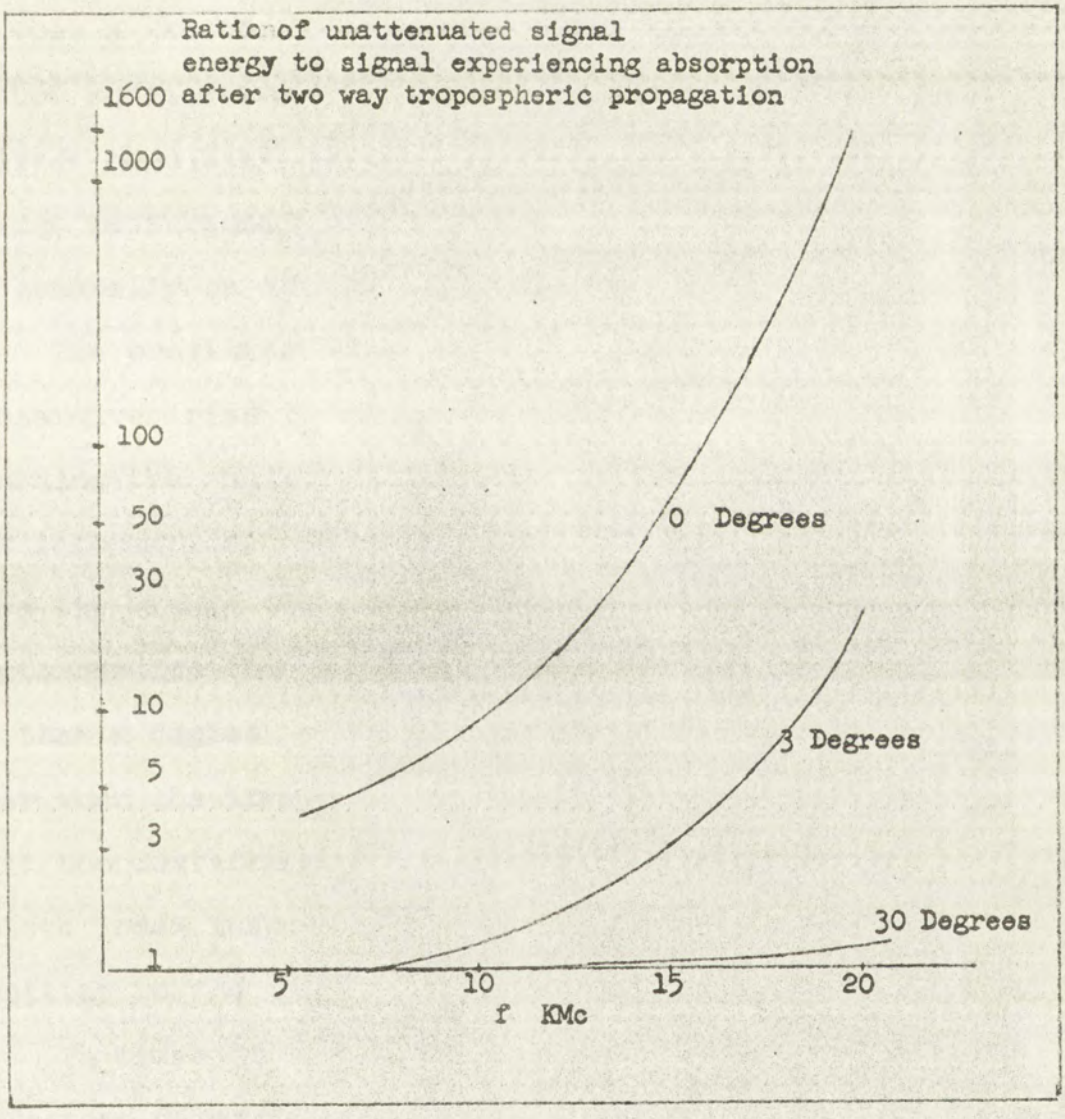

Figure 21

ILLUSTRATION OF ATTENUATION DUE TO ABSORBTION

SUMMARY AND CONCLUSIONS

The present "state-of-the-art" limitation on radar position determination is the refractive effect of the atmosphere. The inherent accuracy of present equipment is such that a "standard" correction for low elevation angles does not suffice and the remaining inaccuracy is of greater magnitude than that introduced by the equipment. The error in range measurement is normally minor and an average correction will generally be adequate.

The precision of measurement evidenced by radars now in use has given rise to the development of accurate means of evaluating the angle and range corrections, given the proper index information. Making use of these correction schemes, errors lie within the radar's precision limitations, even for targets outside the troposphere, except for elevation angles less than a degree. In the extremely low angle range, errors larger than the inherent precision of the radar occur, apparently due to the instantaneous changes in the atmosphere, and incomplete index information. In all cases the accuracy is directly related to the quality of weather information.

In order to evaluate the other effects of the atmosphere, the factors determining the measurement of time lag were investigated. Using the assumption of high signal to noise ratios and the somewhat questionable assumption of no change in signal

waveform, information theory was used to study the parameters affecting accuracy. This development was based on the "inverse probability" of our time delay parameter. Our ideal receiver presents the probability distribution, or an informationally equivalent waveform, of the time lag given the reflected signal and noise. The standard deviation of the time error is shown to be inversely proportional to the square root of the signal to noise ratio and the effective bandwidth. The effective bandwidth should not be confused with the actual physical bandwidth. The effective bandwidth is defined as 2π times the rms deviation in the energy spectrum of our low frequency function about zero frequency.

Where the atmosphere is not frequency sensitive, the refraction of our wave will have no effect on these parameters, and our inherent radar accuracy remains the same.

To determine the sensitivity of the radar's range accuracy to pulse type, the effective bandwidth of rectangular and Gaussian wave shapes was determined. For greatest range accuracy, the use of pulse compression was suggested as it affords a means of increasing the effective bandwidth without increasing the energy. The theoretical range accuracy limitations were roughly an order of magnitude or so better than the practical accuracies presently attainable.

In the vicinity of 15 KMc the atmosphere becomes noticeably frequency sensitive and the question of the continued

validity of our assumption of no change in wave shape, on which our inherent accuracy is based, becomes important. Making use of the complex dispersion equation the variation of the complex inductive capacity with frequency was investigated. This was related to the actual dispersive and absorptive effects of the atmosphere. While the expressions developed were based on simplified theoretical relationships, the agreement with actual absorption measurements is close enough so that the conclusions drawn from the theoretical development are justified.

The development indicated that the error introduced by the dispersion of the wave due to the frequency sensitive atmosphere is generally negligible.

For any long range, accurate tracking requirements at low angles, the absorption will generally limit us to frequencies below 15KMc. The use of masers and lasers at light frequencies opens up a new frequency band for target location and tracking systems. While, with high power ratios, wide bandwidths and low noise equipment we might use frequencies above 15KMc we would have less satisfactory results, and gain no technical advantage from these higher frequencies. The intermittent nature of absorptive scattering due to fog, rain and other precipitation was not considered, but since it becomes more pronounced as the wavelength approaches the size of the particle, it can cause considerable absorption in the vicinity of 15 KMc. This, in conjunction with the molecular

absorption help establish 15KMc as an approximate upper limit for accurate radar tracking over considerable distances.

While not attempted in this report, an interesting application of information theory would be the consideration of the inverse angular determination probability. This would involve such parameters as the beam width, effective aperture, and the signal to noise ratio. By analogy we could again expect the accuracy to be inversely proportional to the signal to noise ratio to the one-half power and accordingly look for a drop in accuracy as we enter the region of high absorption. Since there is no appreciable change in our wave shape below 15 KMc, we would expect the change in signal to noise ratio again to be the most important factor in the determination of accuracy.

APPENDIX A

STRATIFIED ATMOSPHERE REFRACTION CORRECTION METHOD

For a simple approximate estimation of the necessary corrections for atmospheric refraction the atmosphere can be symmetrically stratified in layers of equal index with the geometry as shown in figure A1.

The mathematics involved is simple trigonometry, making use of Snell's Law for spherically symmetrical surfaces.

$$n_1 r_1 \cos i_1 = n_2 r_2 \cos i_2$$

or (A1)

$$n_1 r_1 \sin\alpha_1 = n_2 r_2 \sin\alpha_2$$

The method followed is neither original nor accurate, but considering the error inherent in using the standard atmosphere the results will give approximate trospheric refraction errors, which is the best we can expect without more accurate information.

$$\frac{\sin\alpha_1}{r_1} = \frac{\sin(\frac{\pi}{2} + i_1)}{r_2} \tag{A2}$$

$$i_m = \cos^{-1}\left[\frac{n_{m-1}\, r_{m-1}\, \cos i_{m-1}}{n_m r_m}\right] \tag{A3}$$

$$\alpha_m = \sin^{-1}\left[\frac{r_m}{r_{m+1}} \cos i_m\right] \tag{A4}$$

Applying the law of sines for the direct path

$$\cos i_m = \frac{r_{m+1}}{r_m} \sin\left[\sum_{j=1}^{m} \theta_1\right] \tag{A5}$$

and

$$R_{1m} = r_1^2 + r_{m+1}^2 - 2r_1 r_{m+1} \cos \left[\sum_{j=1}^{m} \theta_j \right] \quad (A6)$$

where

$$\theta_j = \frac{\pi}{2} - \alpha_j - i_j$$

The refraction angle error then is $\Delta i = i_1 - i_m$
and the range error is determined as follows:

$$t_j = \frac{R_j}{V_j} = \frac{n_j}{c} R_j \quad (A7)$$

$$T = \sum_{j=1}^{m} t_j = \frac{1}{c} \sum_{j=1}^{m} n_j R_j \quad (A8)$$

Some average velocity has been calibrated into the radar so that its determination of T will result in a range $R = T V_a$
Therefore,

$$\Delta R = \frac{V_a}{c} \sum_{j=1}^{m} n_j R_j - R_{1m} \quad (A9)$$

If the free space velocity c has been calibrated into the radar then,

$$\Delta R = \sum_{j=1}^{m} n_j R_j - R_{1m} \quad (A10)$$

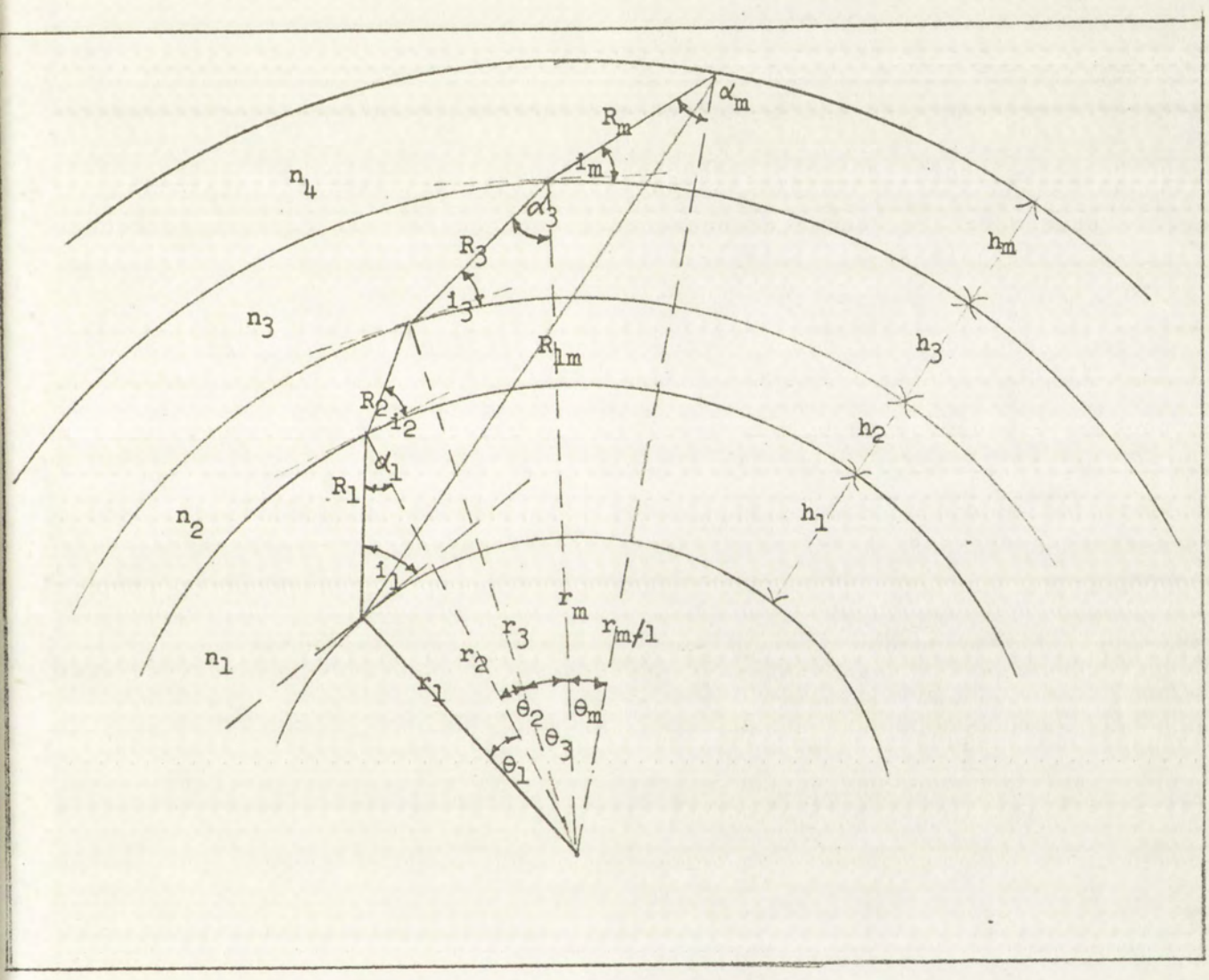

FIGURE 1A

GEOMETRY OF STRATIFIED LAYERS OF CONSTANT INDEX